VARIABILITY IN HOMEOSTATIC TUNING RULES PRODUCES DIVERSE CORRELATIONS IN ION CHANNELS

ROBERT TROMM

Bachelor's Thesis

Presented to

The Faculty of the School of Arts and Sciences
Brandeis University
Interdepartmental Program in Neuroscience
Eve Marder, Advisor

In Partial Fulfillment
of the Requirements for the Degree
Bachelor of Science
in
Neuroscience

by
Robert Tromm

May 2020

ABSTRACT

Neurons are capable of maintaining consistent activity over a long time scale, while undergoing perturbations from factors such as ion channel turnover and activity perturbations. Activity-dependent feedback has been proposed as a homeostatic regulatory mechanism that can regulate channel densities according to the firing rate activity of the neuron. Homeostatic regulation rules can impose correlations on the mRNA- and maximal conductance-level steady state distribution of ion channels. However, it is not currently known how these tuning rules result in the emergence of ion channel correlations. This thesis explores how variability in the parameters of homeostatic tuning rules, such as intracellular Ca^{2+} concentration targets, transcription rates, and translation rates can result in the emergence of diverse, robust correlations between ion channels in neurons.

"A self-organizing system acts autonomously, as if the interconnecting components had a single mind. And as these components spontaneously march to the beat of their own drummer, they organize, adapt, and evolve toward a greater complexity than one would ever expect just by looking at the parts by themselves."

— L. K. Samuels [46]

ACKNOWLEDGMENTS

I would like to thank everyone who has graciously provided me with their support and validation through the entire process of writing this thesis. Thank you to Srinivas Gorur-Shandilya, who made all of this possible and encouraged me to pursue this, despite everything. Thank you to Eve Marder who took me in and, without asking, re-arranged my life and education in ways I will forever be grateful for.

I could not have done this without my family, either. Thank you to Sophia, Bobby, Nikki, Miles, Hayden, and Cam. And finally, thank you to my chosen family. Thank you to everyone who has spent countless hours with me talking and philosophizing about science and the world, to everyone who has pushed me to be better than I am now, and most importantly, made the choice to love and support me in ways I will forever remember and be grateful for.

CONTENTS

1 INTRODUCTION 1
- 1.1 Homeostasis 1
- 1.2 Ion Channel Correlations 3
  - 1.2.1 Degeneracy 4
  - 1.2.2 Homeostasis & Ion Channel Correlations 5

2 METHODS 11
- 2.1 Neurodynamics 12
- 2.2 Homeostatic Rules 13
- 2.3 Model Parameters 14
- 2.4 Simulating Neurons 16
- 2.5 Initial Conditions 16
- 2.6 Activity Metrics 17
- 2.7 Model Implementation 17

3 RESULTS 18
- 3.1 Variability in Initial Conditions of Model Neurons 20
- 3.2 Variability in Passive Ion Leak Conductance 24
- 3.3 Variability in Target Ca^{2+} Concentration 26
- 3.4 Variability in Controller Translation Time Constant 28
- 3.5 Variability in Controller Transcription Time Constant 30

4 CONCLUSION 33

BIBLIOGRAPHY 35

LIST OF FIGURES

Figure 1.1 Variation in K^+ currents and K^+-type maximal conductances in neurons in the stomatogastric ganglion (STG). 2
Figure 1.2 Correlations between 13 ion channel mRNAs in PD neurons. 4
Figure 1.4 Model of activity-dependent feedback. 6
Figure 1.5 Activity pattern differentiation in a single Ca^{2+} sensor setup. 7
Figure 1.6 Activity pattern differentiation in a multiple Ca^{2+} sensor setup 8
Figure 1.3 Dependence of different patterns of activity on ion channel relationships. 10
Figure 2.1 Circuit diagram representing membrane of a neuron. 11
Figure 3.1 Development of an integral control model. 19
Figure 3.2 Mean ion channel conductances of initial conductance values (g_o) and steady-state maximal conductance values in an integral control model. 20
Figure 3.3 Correlations between ion channels after homeostatic regulation. 21
Figure 3.4 Variability in initial maximal conductances and mRNA levels under integral control. 23
Figure 3.5 Variability in passive ion leak conductance (g_{leak}) under integral control. 25
Figure 3.6 Variability in Ca_{target} under integral control. 27
Figure 3.7 Variability in τ_g under integral control. 29
Figure 3.8 Variability in τ_m under integral control. 31

LIST OF TABLES

Table 2.1 Reversal potentials for each ion channel. 14
Table 2.2 Integral control model parameters 15

ACRONYMS

STG	stomatogastric ganglion
PD	pyloric dilator
CG	cardiac ganglion
LP	lateral pyloric
IC	inferior cardiac
g_{NaV}	fast sodium conductance
g_{CaS}	slow calcium conductance
I_{Ca}	calcium current
g_{A}	fast transient potassium conductance
g_{KCa}	calcium-dependent potassium conductance
g_{Kd}	delayed rectifier potassium conductance
g_{K}	general potassium conductance
g_{H}	hyperpolarization-activated mixed-cation inward conductance
g_{leak}	passive ion leak conductance
I_{NaV}	fast sodium current
I_{CaT}	fast transient calcium current
I_{CaS}	slow calcium current
I_{A}	fast transient potassium current
I_{KCa}	calcium-dependent potassium current
I_{Kd}	delayed rectifier potassium current
I_{H}	hyperpolarization-activated mixed-cation inward current
I_{leak}	passive ion leak current
g_{o}	initial conductance values
Ca_{target}	calcium target
τ_{m}	controller transcription time constant
τ_{g}	controller translation time constant
V_{m}	membrane potential
Cm	specific membrane capacitance

1 INTRODUCTION

Neurons are capable of taking in, integrating, and outputting an enormous variety of information. Neurons can communicate information regarding everything ranging from motor behavior to complex sensory input, decision-making, and cognition. This requires neurons to be highly sensitive to internal cues such as intended modulation via biochemical and electrical pathways. On the other hand, neurons must maintain a consistent pattern of activity over a long timescale, despite high variability in intrinsic properties of neurons of the same type, and environmental perturbations such as ion channel turnover and activity perturbations. Neurons maintain this activity through homeostatic regulation, which is carried out through the use of neuromodulation and activity-dependent feedback[8, 12, 24, 25, 27, 28, 66, 69].

Previous work has described the existence of correlations between ion channel maximal conductances and channel mRNA concentrations in neurons[17, 48, 49]. Correlations are highly variable across neurons of the same cell type, but sets of correlations can be characterized to accurately predict the behavioral activity of a neuron. Correlations between ion channels have been shown to emerge from homeostatic tuning rules[36], and may provide a mechanism by which homeostatic regulation can maintain consistent activity while neurons are undergoing ion channel turnover[37]. However, it is currently unknown how homeostatic regulation can produce ion channel correlations. In this thesis, we will explore the possible mechanisms by which homeostatic tuning rules can produce ion channel correlations by modulating individual aspects of a model of homeostatic regulation.

1.1 HOMEOSTASIS

Neurons maintain reliable patterns of activity despite high variability within neurons of the same type and a variety of external perturbations[12, 17, 24, 62–65]. For example, loss of neuromodulatory input is associated with changes in intrinsic membrane conductances which result in restoration of target firing rate activity[64, 65]. Acting in synergy with their respective neuromodulatory environments, cells can stabilize activity over a long timescale[15, 38]. The process of stabilizing electrical activity is undertaken by the use of compensatory mechanisms which make the neuron robust to perturbation. These mechanisms widen the range of characteristic sets of mRNA levels and conductance densities that produce desired activity[16, 45]. Figure 1.1 provides an example of this feature. For two different inferior

cardiac (IC) neurons in the stomatogastric ganglion (STG), there exists significant variability between the two cells in their respective K^+ currents and maximal conductance values. It can be seen here that individual channel maximal conductances vary several-fold in their respective densities. Despite this wide variation in ion channel maximal conductances, these neurons all produce the same patterns of activity.

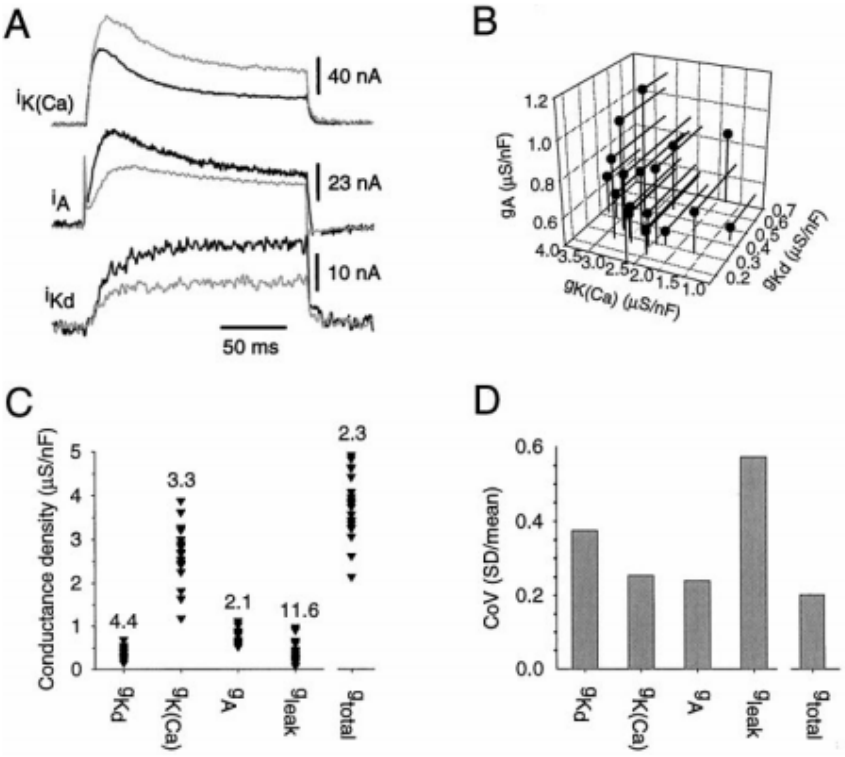

Figure 1.1: IC neurons in the STG show significant variability in K^+ currents and K^+-type channel maximal conductances[17]. (A) shows an example of three K^+ currents in two different IC neurons. (B) shows the mutual relationship between three different K^+-type channel maximal conductances. (C) Variation in conductance densities of K^+-type maximal conductances and the respective ratios between maximum and minimum conductance densities. (D:) Coefficient of variation (CoV) for the same K^+-type channel maximal conductances as in (C:). Figure reproduced from [17].

Previous work has shown that homeostasis in neurons can be regulated by a target level of excitability, which can be regulated by neuromodulation and activity-dependent feedback[8, 12, 24, 25, 27, 28, 66, 69]. Both mechanisms have been shown to be necessary for regulation of firing rate activity[59]. These mechanisms can change ion channel properties such as maximal conductance densities and mRNA transcript levels, in turn modulating firing rate activity[9, 34, 69]. Furthermore, the processes can modulate spatial distribution and

localization of ion channels as well as associate channels with subunits that can further modify them[23, 33, 35, 51].

This thesis will utilize activity-dependent feedback as a homeostatic compensatory mechanism to explore the possible mechanisms which produce a wide variation in ion channel maximal conductances. Activity-dependent feedback is premised on the idea that control of ion channel turnover must be regulated by a mechanism which is reliant on the firing properties of the neuron[24, 27, 55]. It has been shown to produce compensatory changes in ion channel maximal conductance densities and mRNA concentrations after prolonged changes in firing rate activity[9, 19, 59, 64, 65]. This has been in observed in an experimental setting. For example, lobster STG neurons which were chronically isolated from modulatory input recover endogenous bursting due to changes in intrinsic membrane conductances, indicating the presence of an activity-dependent mechanism[64, 65]. Theoretical work has also shown that activity-dependent feedback can allow model neurons to produce complex patterns of activity starting from initial channel maximal conductances that produce quiescent behavior on their own[24, 27, 36]. These conductance-based models produce desired behavior via changes in conductance expression that are a result of activity-dependent cell-type specific channel expression rates.[37].

1.2 ION CHANNEL CORRELATIONS

Homeostatic regulation has been shown to produce diverse, highly variable correlations between ion channels[17, 48, 49]. These correlations between ion channel maximal conductance densities and mRNA levels are found across phyla, and have shown to not be more similar within an animal than across a population, indicating genetic conservation of ion channel correlations[60, 61].

Examples of ion channel correlations are well documented within cell types and across species[30, 47, 48]. For example, correlations have been shown to exist in the cardiac ganglion (CG), as well as the STG in crustaceans[3, 48, 49, 60]. Figure 1.2 shows a correlation network plot between thirteen different ion channel mRNAs in 11 pyloric dilator (PD) neurons in the STG. Correlations are highly varied, exhibiting differences in connectivity and connection strengths between different mRNA levels.

Along with that, changes in maximal conductances or mRNA levels of one ion channel can result in compensatory changes in others to preserve the activity of the neuron. For example, removal of I_{Ca} causes compensatory decreases in I_{KCa} and I_A that are independent of kinetic channel properties[39]. Along with that, in the PD neurons in the STG, there exist strong correlations between channel conductance densities, as well as between mRNA levels, and the two have considerable overlap[58]. These findings exemplify that homeostatic regulation can

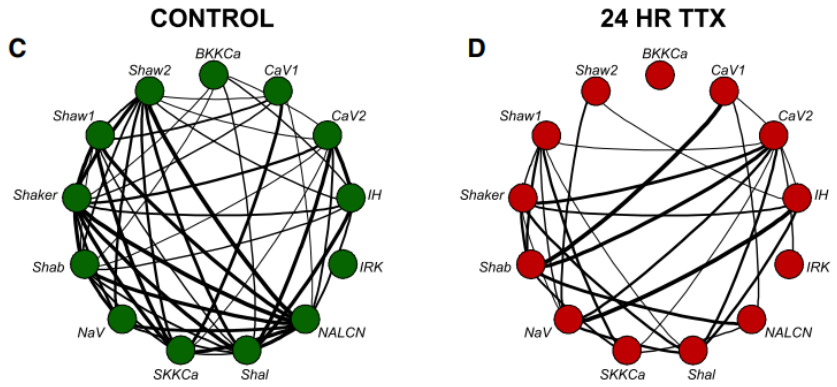

Figure 1.2: Correlation network plot of relationships between 13 ion channel mRNAs in eleven PD neurons in the STG. Correlations between ion channel mRNAs are shown to be vary significantly in connectivity and connection strength, indicated by the varying thickness of lines between ion channel mRNAs. (C:) Correlations between ion channel mRNAs in control. (D:) Correlations between ion channel mRNAs after 24 hours of tetrodotoxin (TTX) application. Correlations change significantly after application. Some relationships are totally lost (e.g. *BKKCa* and *Shaker*), while some are strengthened by application of TTX (e.g. *CaV1* and *Shab*). Figure reproduced from [47].

produce ion channel correlations and that correlations can make the neuron robust to perturbation by providing a mechanism by which neurons can up- or down-regulate ion channels dependent on the activity of its correlated channels.

1.2.1 *Degeneracy*

Membrane channel mRNA levels and conductance density values can vary several-fold across cells of the same type[17, 27, 41, 49, 56]. It has been shown that this phenomenon occurs across species and types of neurons, ranging from neurons in the STG to Purkinje cells in the cerebellum, and dopaminergic cells in the substantia nigra[26, 49, 56]. For example, K^+ currents in IC neurons in *Cancer borealis* display two- to five-fold variation in current densities[17]. This indicates that neurons are degenerate with respect to patterns of activity – behavioral patterns cannot be specified by a single set of maximal conductance densities or mRNA levels. Rather, it has been shown that multiple sets of correlated ion channel mRNA levels and conductance densities can be characterized to identify neuronal cell types[36, 37, 48].

From examination of these sets of parameters, it becomes clear that there are patterns of correlations between individual ion channels that are consistent across sets of ion channel maximal conductances and mRNA levels that produce the same patterns of activity. For example,

hyperpolarization-activated mixed-cation inward conductance (g_H) and fast transient potassium conductance (g_A) channel types consistently occur in a set ratio in their amplitudes[29, 30]. Along with that, PD neurons and lateral pyloric (LP) neurons have been shown to possess correlated levels of g_H, g_A, and calcium-dependent potassium conductance (g_{KCa}), and are altered in a cell-specific manner by perturbation[50, 58]. Figure 1.3 shows the dependence of activity on both individual and subsets of ion channel maximal conductances. It can be seen that the same maximal conductance in one ion channel can result in different behavior depending on its relationship to maximal conductance densities of the other ion channels.

These patterns of correlations in channel expression and conductance density have been proposed reflect the tuning of conductances required to maintain target activity over a long period of time[31, 49]. This may arise during all periods of the life of a neuron, or it may be specific to initial development. In the STG, it has been proposed that tuning rules governing development of neurons may result in networks that are highly variable across individuals by the time neural networks are fully developed[32, 43, 44]. Furthermore, variability in other systems may induce variability in ion channel expression and current densities – the variability of transcriptional machinery and regulatory transcriptional sequences can lead to variability in gene transcription, and subsequently ion channel expression[6, 68]. It is currently unknown what biological mechanism, or mechanisms, produce variability across ion channel mRNAs and maximal conductance densities. Though neuroscience has come a long way in understanding how characteristic sets of ion channel mRNAs and maximal conductances can produce similar patterns of activity, we still do not know what drives the existence of these correlations[41].

1.2.2 *Homeostasis & Ion Channel Correlations*

The existence of correlations between membrane ion channels may represent a mechanism by which homeostatic regulatory features may enforce and stabilize desired activity in specific neurons[48]. Co-regulation of ion channels can theoretically prevent loss of activity while the neuron is being affected by environmental perturbations such as ion channel turnover and activity perturbations[5, 30, 36]. Characteristic sets of ion channel correlations can consistently produce desired firing rate activity despite high variability in levels of channel conductance densities between individual neurons of the same cell type. This has been proposed to occur through the enforcement of ion channel ratios, which are correlated to specific activity features. This can simplify homeostatic mechanisms and make the neuron robust to perturbations in any one ion channel[2, 7, 29, 48].

Experimental work has shown ion channel correlations to be significantly affected by homeostatic activity[4, 53, 54, 57, 58, 61]. For example, MacLean *et al.* showed that modulating g_A current densities or g_H current densities alone would change the functional output of the neuron, but that modulating both maintained desired functional output[29]. Along with that, inhibition of g_A results in compensatory increase in g_{KCa} that is dependent on intracellular calcium concentration and calcineurin activity[42]. The dependence of this compensatory mechanism on calcium concentration provides evidence that activity-dependent feedback can influence ion channel correlations[64, 65].

Though co-regulation of ion channels provides an avenue by which neurons may maintain desired activity, the mechanism which drives the existence of co-regulation remains a mystery. Activity-dependent feedback represents but one proposed solution. The mechanism not only influences correlations, but is has been found necessary for the existence of correlated ion channels in the STG. Temporal *et al.* performed experiments decoupling activity, synaptic connectivity, and neuromodulatory states of individual neurons from the STG, and found that loss of neuromodulation was not sufficient to result in loss of correlations across channel mRNAs, but loss of activity resulted in loss of all correlations. Thus, it was shown that activity-dependent processes, but not neuromodulatory processes, can dynamically maintain distinct relationships across channel mRNAs in the STG[59]. Activity-dependent feedback mechanisms can generate and regulate biophysically realistic dynamics of neurons in the STG[24, 27, 36, 37]. Figure 1.4 shows how a model of activity-dependent feedback (described in Section 2.2) can produce desired neuronal dynamics by varying channel conductances over time which are dependent on Ca^{2+} dynamics[36].

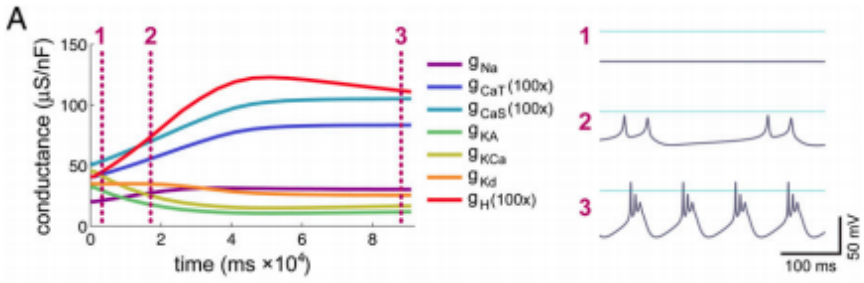

Figure 1.4: Development of channel conductances and patterns of activity at different time-points. (LEFT:) A model of activity-dependent feedback varies channel conductances over time, resulting in desired functional output when channel conductances reach their respective steady-state values. (RIGHT:) Patterns of activity (1-3) correspond to channel conductance values at three points in their evolution over time[36].

These mechanisms are able to reliably influence co-regulation of ion channel pairs over different timescales by changing the properties

of correlations, including slope, strength, and set-points within the parameter space[53, 54, 58, 61]. The key feature of activity-dependent feedback is the dependence of functional output on firing rate activity. To sense changes in firing rate activity, models of activity-dependent feedback must have the capacity to sense these changes. Calcium dynamics have been proposed as a way neurons can sense changes in activity. Calcium dynamics can indirectly express membrane potential (V_m) by simulating the interaction between changes in intracellular Ca^{2+} concentration and changes in V_m.

Modern models of homeostasis typically use calcium dynamics as a sensor by which neurons can regulate activity[27, 36, 64, 65]. Changes in intracellular Ca^{2+} concentration can be averaged over different timescales in order to target different aspects of firing rate activity[27]. In doing so, neurons can assure that functional output is properly maintained. Liu *et al.* described how different patterns of activity can have average Ca^{2+} concentration levels that may be difficult to differentiate between.

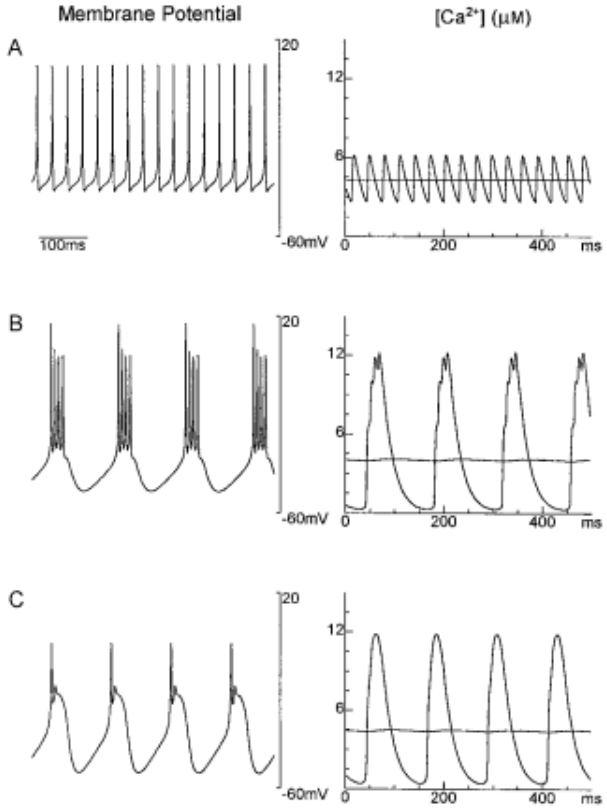

Figure 1.5: Three different patterns of activity have effectively equal average Ca^{2+}. (A:) V_m of a neuron firing tonically. (B:) V_m of a neuron firing with bursting behavior. (C:) V_m of a neuron firing with a different bursting behavior. (ALL, RIGHT:) Instantaneous Ca^{2+} concentration and respective time-averaged values[27].

Figure 1.5 shows that the Ca^{2+} average levels averaged over a single timescale across a tonic firing pattern and two separate bursting patterns are effectively equal. This shows that neurons which use a single Ca^{2+} sensor averaged over one unique timescale can, in theory and in some cases, not differentiate between different patterns of activity. In contrast, Figure 1.6 describes the use of three separate Ca^{2+} sensors which can distinguish between different activity patterns by averaging intracellular Ca^{2+} concentration over three distinct timescales. The use of three sensors is not arbitrary in this case, but targets three key features of the neuron's electrophysiology. The fast Ca^{2+} sensor is able to detect tonic firing patterns, the slow Ca^{2+} sensor is able to detect bursting behavior, and the DC Ca^{2+} sensor can detect slow-wave activity.

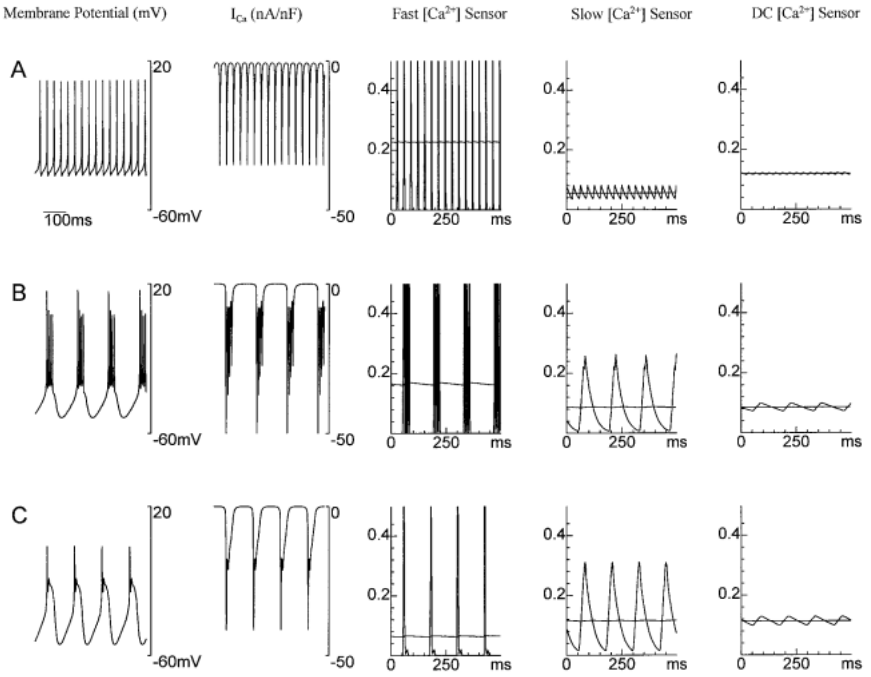

Figure 1.6: Three different Ca^{2+} sensors can differentiate between different patterns of activity. Rows A-C are the same activity patterns found in Figure 1.5. Second column shows Ca^{2+} current. Last three columns show transient and average values for three different Ca^{2+} sensors: Fast, Slow, and DC[27].

Despite this, models of activity-dependent feedback have been produced which can differentiate between different patterns of activity, and reliably produce target behavior from initial conditions which produce quiescent behavior[36, 37]. O'Leary *et al.* has proposed a model which relies on a single Ca^{2+} sensor. At each discrete time-step, the difference, or "error," between the average Ca^{2+} concentration and the target Ca^{2+} concentration is computed, and integrated with past computations of error[37]. This is then fed into two differential equations, one of which represents the synthesis of correlated ion channel

mRNAs, and the other represents translation of ion channel proteins from the current channel mRNA concentration. This model scales the average Ca^{2+} concentration at the level of mRNA transcription, rather than at the level of the Ca^{2+} sensor. Ratios between ion channel maximal conductances can then specify correlations between conductances, and in turn specify the pattern of activity of the neuron. This model is shown to be a perfect candidate for exploring the effect of variability in other properties of the neuron on the variability of ion channel mRNA concentrations and maximal conductance densities.

Despite these significant achievements in producing biophysically realistic models of neuronal dynamics and homeostatic activity, ion channel correlations have nonetheless proven a significant challenge to models of neurons with homeostatic regulation. Sets of correlations are dissimilar across cell types and highly variable within cell types, making generalizability a challenge. Without an understanding of the functional mechanism driving their existence, or the biological mechanisms underlying activity-dependent feedback, creating biophysically realistic models is even more difficult[48]. The experimentally-derived correlations between ion channels have, as of now, not been successfully reproduced in models of homeostatic regulation[27, 36, 37, 48, 49]. The model by O'Leary *et al.* described above is capable of producing linear pairwise correlations between ion channel maximal conductances, but has not been able thus far to produce the non-binary patterns of correlations seen in Figure 1.2[37].

In this thesis, variability in properties of model neurons including initial channel maximal conductances and mRNA levels, passive ion leak conductance (g_{leak}), controller transcription time constant (τ_m), controller translation time constant (τ_g), and calcium target (Ca_{target}) will be varied independently and systematically examined. The purpose in doing this is to understand the influence of intrinsic neural parameters and parameters of homeostatic regulation on emergence of ion channel correlations and the possible ways neurons can manifest ion channel correlations which are as diverse and robust as is seen in experimental observations.[48, 49].

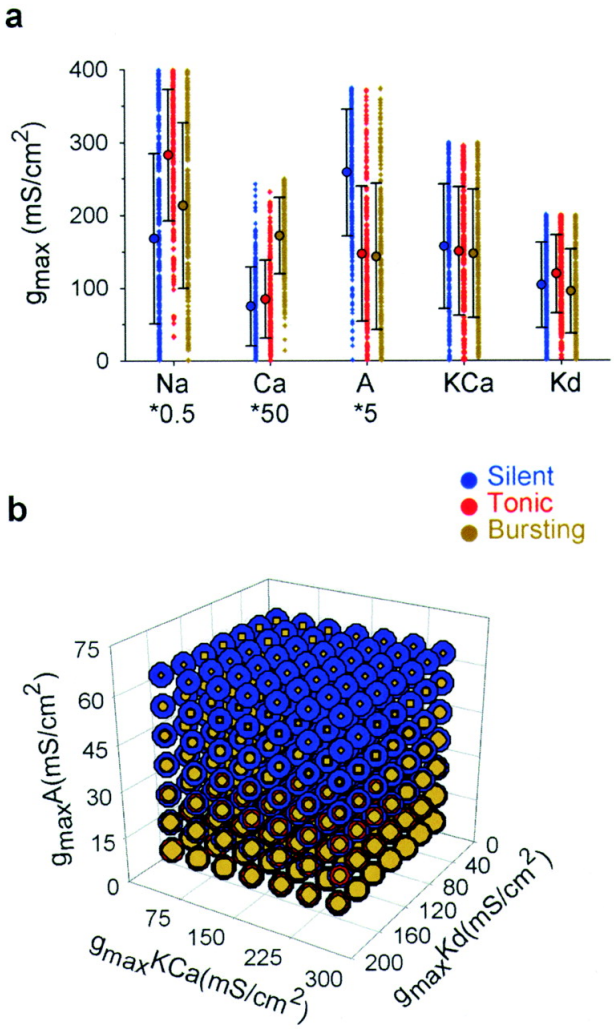

Figure 1.3: Production of different patterns of activity in the neuron is dependent on the relationship between ion channel maximal conductances. The same maximal conductance density in one ion channel can produce unique patterns of activity dependent on its relationship to other channels. (A:) Different states of activity are observed when ion channel maximal conductances are varied over a wide range. (B:) Different patterns of activity emerge from characteristic sets of K^+-type ion channel maximal conductances in a probabilistic manner. The probability of seeing bursting activity, for example, increases as g_A and delayed rectifier potassium conductance (g_{Kd}) decrease toward zero[16].

2

METHODS

This thesis relies on a previously described model of a neuron. It is a single-compartment, conductance-based neuron which is based on the Hogkin-Huxley formalism[20–22]. Previous work has utilized this model neuron as a backbone for exploration of homeostatic compensatory mechanisms[27, 36, 37]. This model represents the neuron as a circuit[20]. Figure 2.1 details the circuit diagram of the neuron as a representation of the cell membrane acting as a capacitor with various ion channels as resistors. The membrane takes in current from the outside, which can be described in more detail as the neuron's neuromodulatory environment.

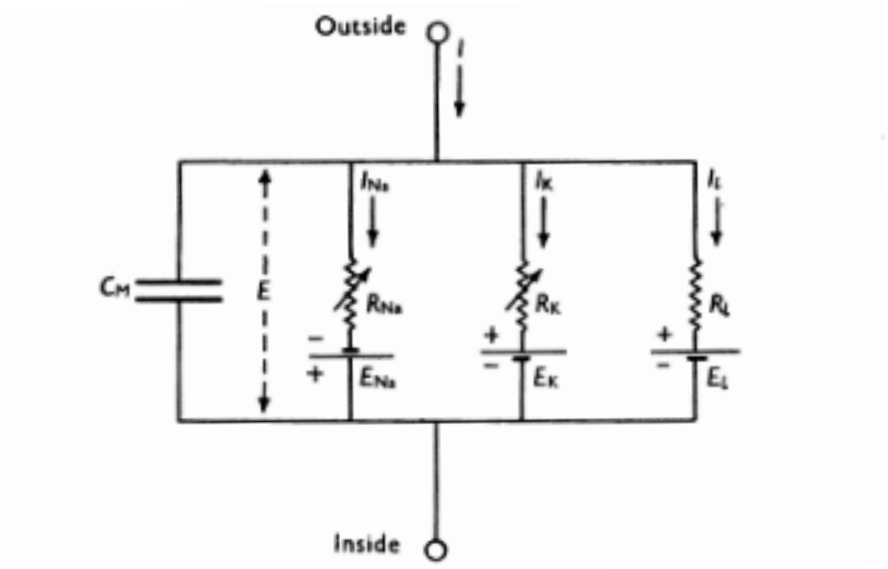

Figure 2.1: Circuit diagram representing the membrane of a neuron. specific membrane capacitance (C_m) represents the total capacitance of the neuron. Resistors represent $1/g_{NaV}$, $1/g_K$, and $1/g_{leak}$[20].

The model neuron has eight transmembrane currents and associated conductances: fast sodium current (I_{NaV}), fast transient potassium current (I_A), hyperpolarization-activated mixed-cation inward current (I_H), calcium-dependent potassium current (I_{KCa}), delayed rectifier potassium current (I_{Kd}), slow calcium current (I_{CaS}), fast transient calcium current (I_{CaT}), and passive ion leak current (I_{leak}). The associated maximal conductances of the first seven transmembrane currents are regulated by the integral control scheme mentioned in Section 2.2. g_{leak} is not regulated in this model.

2.1 NEURODYNAMICS

Neurons are considered to consist of a single compartment, acting as a capacitor, with various ionic currents acting as resistors in parallel, and a specific surface area (in units mm^2). The compartment has a membrane potential (V_m), which evolves according to the equation:

$$C_m \frac{dV_m}{dt} = \sum_i I_i \tag{2.1}$$

where Cm is the specific capacitance of the membrane and I_i is each ionic current in the neuron[18]. Current is given by the equation

$$I_i = g_i(V)(V - E_i) \tag{2.2}$$

where $g_i(V)$ is instantaneous conductance and E_i is the reversal potential (Nernst potential) for each ion channel[18]. Reversal potentials for each ion channel, excluding Ca^{2+}-dependent channels, are considered constant and are described in Section 2.3. This simplification is justified by the law of large numbers – intracellular and extracellular ion concentration are saturated, resulting in effectively constant flux of ions in and out of the cell[27]. Instantaneous conductance $g_i(V)$ is defined by the equation:

$$g_i(V) = \bar{g}_i m_i^{p_i} h_i^{q_i} \tag{2.3}$$

where

$\bar{g}_i$	maximal conductance for each ion channel
m	activation gating variable
h	inactivation gating variable
p, q	integers

The integers p and q are bound by an interval $[0, 1]$[18]. The activation and inactivation variables are themselves defined by an ordinary differential equation which depends on V_m, and is specific to each conductance. The general form is:

$$\tau_m \frac{dm}{dt} = m_\infty - m \tag{2.4}$$

$$\tau_h \frac{dh}{dt} = h_\infty - h \tag{2.5}$$

where τ_m and τ_h are time constants and m_∞ and h_∞ are steady-state values of the activation and inactivation variables[40]. Each conductance has a characteristic steady-state density and time constant which represent its function in the overall neurodynamics of the neuron.

2.2 HOMEOSTATIC RULES

Regulation of firing rate activity in this thesis will rely on an activity-dependent feedback mechanism for regulating ion channel maximal conductances[27, 36, 37, 40]. This mechanism relies on calcium as a sensor, by which neurons may regulate their activity. Section 1.2.2 provides an explanation of the use of calcium ions as an indirect representation of V_m activity. Calcium dynamics in this model evolve according to the equation:

$$\tau_{Ca}\frac{d[Ca^{2+}]}{dt} = -f(I_{CaT} + I_{CaS}) - [Ca^{2+}] + [Ca^{2+}]_0 \tag{2.6}$$

where τ_{Ca} is the time constant, f translates Ca^{2+} current into an intracellular concentration change, and $[Ca^{2+}]_0$ is the steady state intracellular Ca^{2+} concentration if there is no flux of calcium ions across the membrane[27, 40].

The activity-dependent feedback mechanism is based on regulation by a calcium-dependent homeostatic rule, first implemented by O'Leary *et al.*[37]. Regulation of maximal conductances is simulated by two integral control equations:

$$\tau_i \dot{m}_i = [Ca^{2+}] - Ca_{tgt} \tag{2.7}$$

$$\tau_g \dot{g}_i = m_i - g_i \tag{2.8}$$

where τ_i represents the transcription timescale for each ion channel, τ_g represents global transcription timescale, m_i represents mRNA levels for each ion channel, and Ca_{tgt} represents global Ca^{2+} target concentration. Variables are bounded at 0 to ensure that conductances do not become negative.

In this model, Ca^{2+} acts as a feedback control signal. It is purposefully simple, focusing on the essential biological principles underlying formation and degradation of ion channel proteins. Obviously, neurons possess a significant number of other mechanisms of regulation, such as co-trafficking of ion channels, cotranslational interaction, RNA interference, and the use of promoters[1, 14, 37, 52, 67, 70]. Occam's razor dictates that "the simplest solution is most likely the right one," and we will use this as a guideline moving forward.

Steady-state values of m_i are found to be dependent on the time integral of average $[Ca^{2+}]$ and scaled by the inverse of the time constant for the channel τ_i. We can then estimate steady state g_i for very small initial conductance values and positive time constants. We can see this by taking the integral of Equation 2.7:

$$g_i \approx m_i = \frac{1}{\tau_i}\int_0^{t_{ss}} ([Ca^{2+}] - Ca_tgt)dt \tag{2.9}$$

Figure 2.9 also shows how correlations between ion channels emerge when m_i converges to the value dependent on the time integral of average $[Ca^{2+}]$. When one takes ratios between channels, the integrals cancel out, so that:

$$\frac{g_i}{g_j} \approx \frac{\tau_j}{\tau_i} \tag{2.10}$$

It can be seen here that different ratios of the time constants determine the correlations between ion channel conductances. These ratios can determine the electrophysiological character of the neuron, as is further discussed in Section 1.2.2.

2.3 MODEL PARAMETERS

Model parameters are adapted from previous work, and are used as the basis for variation in each experiment presented in this thesis[27, 37, 40].

Each ionic current has its own reversal potential. These values dictate the membrane potential at which ions begin to move in the opposite direction.

CURRENT	I_{NaV}	I_A	I_H	I_{Kd}	I_{KCa}	I_{leak}
$E(\text{mV})$	+50	-80	-20	-80	-80	-50

Table 2.1: Reversal potential for each ionic current. Reversal potential of I_{CaT} and I_{CaS} are not constant and derived from the Nernst potential.[40]

V_m evolves with time according to Equation 2.1 where specific membrane capacitance $C_m = 0.628nF$[20].

Ca^{2+} concentration is dynamic, evolving according to Equation 2.6, where

$\tau_{Ca} = 200ms$

$f = 14.96\mu M/nA$

τ_{Ca} is the calcium buffering time constant, and f is the factor which converts calcium current into intracellular calcium concentration change. This factor depends on the ratio of the surface area of the cell to the volume wherein Ca^{2+} concentration is measured[27]. In this case, volume is considered to be a narrow shell inside the membrane and approximates the neuron by a cylinder $50\mu m$ in diameter and $400\mu m$ long. Surface area of the cell is 0.0628 mm^2[27].

Reversal potentials of Ca^{2+} current types are dependent on voltage and calcium, and are dynamically updated by the Nernst equation[27]:

$$E_{Ca} = \frac{RT}{zF} ln(\frac{[Ca^{2+}]_{ext}}{[Ca^{2+}]_{in}} \tag{2.11}$$

where E_{Ca} refers to reversal potentials for I_{CaS} and I_{CaT}, gas constant $R = 8.314J * mol/K$, temperature $T = 284.15K$, ion charge $z = 2$ for calcium ions, Faraday constant $F = 96485C/mol$, $[Ca^{2+}]_{in}$ is the current intracellular calcium concentration, and the extracellular calcium concentration $[Ca^{2+}]_{ext} = 0.05\mu M$[40].

Voltage-dependent equations for the model parameters for each current were adapted from [40]. Each ionic current has its own specific p, steady-state activation variable m_∞, steady-state inactivation variable h_∞, and time constants τ_m and τ_h, respectively. Ionic currents which are not inactivating do not have values for h_∞ or τ_h.

Maximal conductances are dependent on Ca^{2+} concentration and are regulated by Equations 2.7 and 2.8. The time constant for transcriptional rate τ_{m_i} is unique for each maximal conductance and defined by:

$$\tau_{m_i} = \frac{5e6}{g_{\infty_i}} \tag{2.12}$$

where tau_m is in milliseconds and $g_{i\infty}$ represents the steady-state maximal conductance for each ionic channel. Steady-state maximal conductances were originally adapted from Prinz *et al.*[40].

Ion channel	NaV	CaT	CaS	A	H	KCa	Kd	Leak
g_∞ $(\mu S/mm^2)$	$1e3$	25	60	$5e2$	0.1	50	$1e3$	$*$
τ_m (ms)	$5e3$	$2e5$	$\approx 8.33e4$	$1e4$	$5e7$	$1e5$	$5e3$	$*$
τ_g (ms)	$5e3$	$5e3$	$5e3$	$5e3$	$5e3$	$5e3$	$5e3$	$*$

Table 2.2: Default integral control model parameters. g_∞ adapted from Prinz *et al.* to determine transcriptional rate time constants τ_m for each ionic current[40]. Translation rate time constant τ_g is equal across all ionic currents. *Leak is unregulated in this model and thus does not have τ_m or τ_g time constants.

Table 2.2 describes the regulation time constants used in both Equations 2.7 and 2.8. Steady state maximal conductances (g_∞) were computed by simulating a known working set of eight channel maximal conductances adapted from Prinz. *et al.* for $t = 400s$ with a time-step of $dt = 0.1ms$ to ensure all maximal conductances converged at their respective steady state densities[40]. These values are only used to compute the transcription and translation rate time constants, and are not used at any point after these values are calculated. It should be of note that these time constants are the default for all experiments, except in cases where the time constants are being varied themselves. In that case, these default values are used as a median point upon which to build a distribution. Target Ca^{2+} concentration was established for a bursting neuron through this same method. Average Ca^{2+} concentration, averaged over 200ms, was obtained from the model after

simulation. Initialization of Ca^{2+} target concentration and regulation time constants was repeated at the beginning of each experiment.

2.4 SIMULATING NEURONS

Model neurons are simulated according to the exponential Euler method,[11, 18] which approximates V_m at each discrete time step by the equation:

$$V(t + dt) = V_\infty + (V(t) - V_\infty)exp(-\frac{dt}{\tau_V}) \tag{2.13}$$

Neurons are simulated for $t = 200s$ with a timestep of $dt = 0.1ms$. Voltage traces used for figures and metrics are computed by simulating model neurons for $t = 6s$ with a timestep of $dt = 0.1ms$.

The homeostatic mechanism is simulated by the Euler method[18]:

$$Ca_{err} = Ca_{tgt} - Ca_{prev} \tag{2.14}$$

$$m_i(t + dt) = m_i + \frac{dt}{\tau_{m_i}} Ca_{err} \tag{2.15}$$

$$\bar{g}_i(t + dt) = \bar{g}_i + \frac{dt}{\tau_{g_i}}(m_i - \bar{g}A) \tag{2.16}$$

where m_i represents ion channel mRNA concentration for each current, $\bar{g}_i$ represents maximal conductance density for each current, Ca_{tgt} represents target average Ca^{2+} concentration, Ca_{prev} represents Ca^{2+} concentration at the previous time-step, and A represents the surface area of the model neuron.

2.5 INITIAL CONDITIONS

Model compartments are initialized with parameters $V_m = -60mV$ and $[Ca^{2+}_{in}] = 0.05\mu M$. Initial maximal conductances ($\mu S/mm^2$) for each channel (excluding g_{leak}) and compartment mRNA concentration (μM) are varied across all experiments. g_{leak} is held fixed at $\bar{g}_{leak} = 0.05$, except in Figure 3.5. Values are generated for all simulations at the beginning of each experiment by the use of a random number generator scaled by a noise factor. For the first experiment, where initial conditions are varied alone, the noise factor is 20 for channel maximal conductances and 0.004 for compartment mRNA concentration. For all other experiments, the noise factor is 5 for channel maximal conductances and 0.001 for mRNA levels.

2.6 ACTIVITY METRICS

For each simulation, metrics were computed on model parameters to determine if models were working or not. Models were considered to have converged if

$$| \frac{([Ca_{tgt}] - [Ca_{avg}])}{[Ca_{tgt}]} | > 0.1 \tag{2.17}$$

where Ca_{tgt} is the target Ca^{2+} concentration and Ca_{avg} is the average Ca^{2+} concentration after homeostatic regulation.

Models were then checked against reference model with parameters described in Table 2.2. Burst periods and duty cycle were checked against reference model. If the burst period of the tested model deviated from reference by more than 20% or the duty cycle deviated from reference more than 10%, the model was considered nonfunctional.

2.7 MODEL IMPLEMENTATION

Model neurons were implemented using `xolotl` v.20.4.22 and v.20.2.26, an open-source neuron simulator written in C++ for MATLAB[18]. Credit to Srinivas Gorur-Shandilya for development and implementation of the modeling platform. Simulation data was retrieved through the use of MATLAB ver. R2020a.

3

RESULTS

How do homeostatic tuning rules produce variability and correlations between ion channel conductances and mRNA levels in neurons? To answer this question, we will vary intrinsic properties of a model neuron and properties of a homeostatic tuning rule to ascertain the influence of these parameters on the emergence of correlations between ion channels in neurons. We began with a conductance-based model neuron based on the Hogkin-Huxley formalism that was modified to take advantage of a homeostatic compensatory mechanism. Model neurons utilize intracellular Ca^{2+} concentration as a sensor to regulate conductance values of individual ion channels. These neurons are thus indirectly dependent on V_m via the dependence of Ca^{2+} dynamics on V_m[27, 36]. This model produces and maintains complex activity patterns, such as tonic firing and bursting behavior, through the interplay between target Ca^{2+} concentration, Ca^{2+} dynamics, and voltage-dependent ion channels.

We will utilize an integral control model, based off of the mechanism proposed by O'Leary *et al.* which utilizes a single Ca^{2+} sensor to regulate channel mRNA levels and maximal conductances based on firing rate activity.[36]. Rate of regulation of maximal conductance values by the homeostatic rule is based on experimental work suggesting that regulatory dynamics occur over hours or even days[10, 13, 62]. Of course, simulating the evolution of neurodynamics over a period of hours or even days is computationally inefficient, so both the time of integration and regulatory timescales have been scaled down to a more appropriate 200 seconds for each simulation.

Figure 3.1 shows the development of maximal conductances over time. Each individual line in the top section of the figure corresponds to the development of each ion channel maximal conductance. The bottom section shows the functional output of the model before and after homeostatic regulation. Quasi-random initial conditions were generated for initial maximal conductances and ion channel mRNA levels. The model was then allowed to develop in an unconstrained manner for a set period of time ($t = 200s$).

We wanted to understand not only how neurons are capable of producing correlations between ion channels, but how variability in the scale and connection strengths of correlations was produced by homeostatic regulation. We assumed that variability in scale and connection strengths of ion channel correlations is not dependent on the intrinsic parameters of the neuron, but rather the parameters of the homeostatic tuning rule. To answers these questions, we will start by varying initial

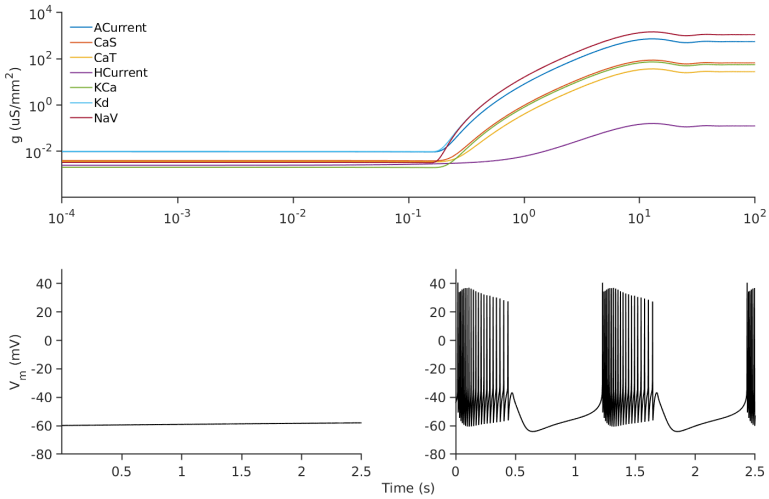

Figure 3.1: An integral control scheme with one Ca^{2+} sensor can produce bursting behavior after homeostatic regulation. (Top:) Development of maximal conductances from initial conditions. g_{leak} is excluded as it is not regulated. (Bottom, left:) Quiescent behavior in model neuron prior to homeostatic regulation. (Bottom, right:) Bursting behavior of model neuron after t = 200 seconds. Integral control scheme adapted from [36].

conditions (channel maximal conductances and mRNA levels) of the model neuron. Then, we will vary passive ion leak conductance (g_{leak}), as it is not regulated by the homeostatic tuning rule. Then, we will vary parameters in the homeostatic tuning rule, including Ca^{2+} target concentration, controller translation time constant (τ_g), and controller transcription time constant (τ_m). Taking into account how variation in intrinsic model neuron parameters affects patterns of correlation, we will systematically examine how variation in these parameters changes the patterns of correlations between steady state channel maximal conductances to ascertain the influence of each parameter on the emergence of ion channel correlations in neurons.

Before modulating the individual parameters of the model, we wanted to recapitulate that the model was capable of producing similar patterns of activity from significantly different sets of initial channel maximal conductances[37]. We initialized two sets of 1000 model neurons each with initial maximal conductance values that differed by 100-fold between distributions. We set target Ca^{2+} concentration to be the reference value for a bursting neuron obtained from the database produced by Prinz *et al.* and described in Section 2.5[40]. We then simulated unconstrained homeostatic regulation for each model neuron for $t = 200s$. We filtered out models where maximal conductances had not converged to steady state, or had bursting periods and duty cycles that differed significantly from the reference model, as further described in Section 2.6. Figure 3.2 shows the mean values of each ion

channel maximal conductance before and after homeostatic regulation for both sets of model neurons. It is shown that despite a 100-fold difference in initial ion channel maximal conductances between sets, the same pattern of steady state maximal conductances emerges after homeostatic regulation in each set of model neurons.

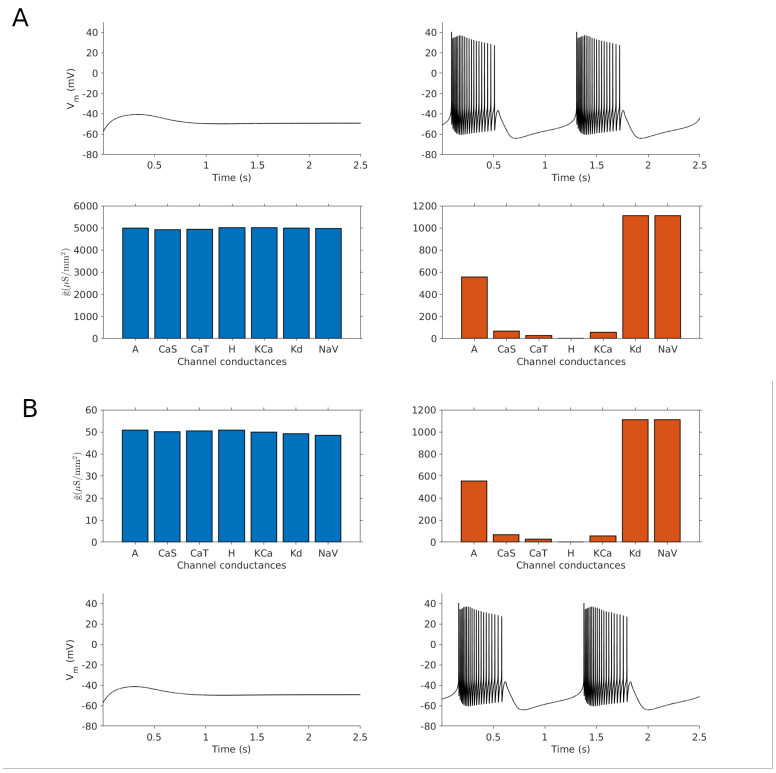

Figure 3.2: A characteristic set of mean steady state maximal conductances (orange) emerges from two significantly different sets of initial mean maximal conductances (blue). Despite a 100-fold difference between the two distributions of initial maximal conductances, a strikingly similar set of steady-state maximal conductances is produced in both cases. Initial conditions were generated by a random number generator scaled by a factor of (A:) 1000 and (B:) 100. Note that g_H is present, but of significantly lower value than other maximal conductances.

3.1 VARIABILITY IN INITIAL CONDITIONS OF MODEL NEURONS

After establishing that the model could reproduce characteristic sets of channel maximal conductances for a target behavior, we wanted to explore the correlations between ion channels after homeostatic regulation. Figure 3.3 shows how pairwise correlations between ion channels emerge from homeostatic regulation utilizing the same integral control scheme described above. 1000 model neurons were initialized with quasi-random initial ion channel maximal conductances varying between [0,5]. After homeostatic regulation, all steady state maximal

conductances converge to a single common plane, indicating that the solution set of all channel maximal conductances that produce target activity can be derived from further analysis of this plane. Furthermore, ion channel maximal conductances in this model are perfectly correlated when initial channel maximal conductances and channel mRNA concentrations are varied by a small degree. It was seen that despite maximal conductances between ion channels existing at different scales, regulated by their individual regulation time constants, an increase in one ion channel maximal conductance is matched by all others at an equal rate.

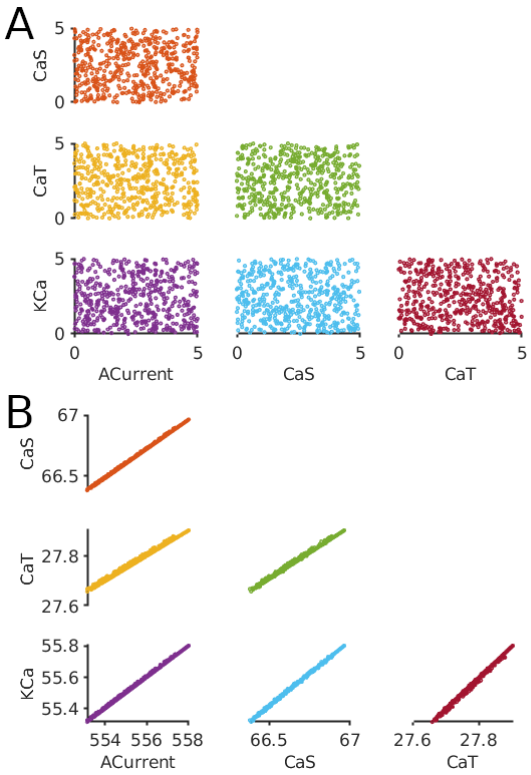

Figure 3.3: Pairwise correlations between ion channel maximal conductances ($\mu S/mm^2$) emerge from a homeostatic regulatory mechanism with one Ca^{2+} sensor. Range of variation for each maximal conductance is less than what has been established in experimental observations[17]. Sets of initial maximal conductances between [0,5] and compartment mRNA concentration between [0,0.001] are not sufficient to reproduce experimentally observed variation in maximal conductances. This small variation in initial conditions reproduces the linear pairwise correlations between steady state maximal conductances seen in [37]. Each data point represents ion channel maximal conductances from one simulation. (A:) Pairwise correlations in initial maximal conductances between ion channels. (B:) Pairwise correlations in steady-state maximal conductances between ion channels.

This result was expected. However, in experimental observations of correlations between channel mRNA concentrations, pairwise correlations between mRNA levels vary several-fold, and have diverse connection strengths which do not result in perfectly correlated steady state maximal conductances. Pairwise correlations between channel mRNAs do not, in all cases, vary at the same rate as each other, and some channels are not correlated at all[47].

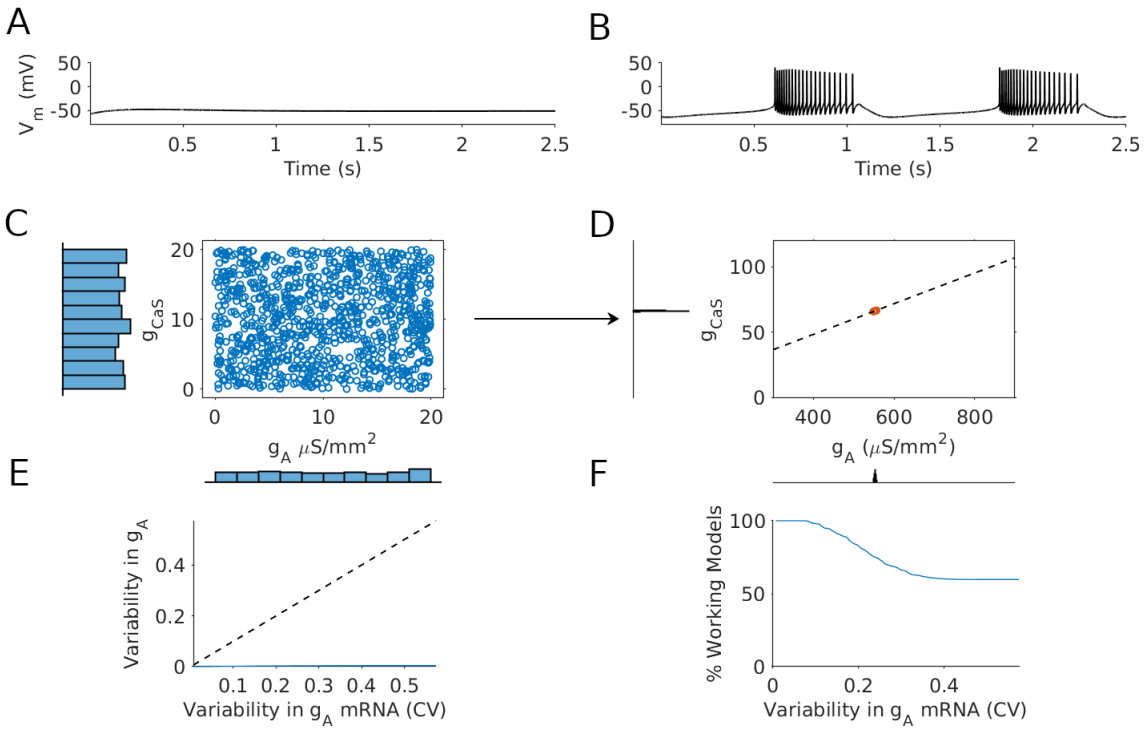

Figure 3.4: Variability in initial maximal conductances and channel mRNA concentration is not sufficient to reproduce experimentally observed variation in maximal conductances. Coefficient of variation (CV) for initial g_A is 0.58, and for steady state g_A is 0.0030. The homeostatic rule is shown here to compress variability in maximal conductances by a factor of 190 when initial maximal conductances and compartment mRNA levels are varied by a factor of 20 and 0.004, respectively. (A:) Voltage trace of model neuron prior to integration shows quiescent behavior. (B:) Voltage trace of model after integration shows bursting behavior. (C:) Pairwise correlations between g_A and slow calcium conductance (g_{CaS}) prior to integration. (D:) Pairwise correlations between g_A and g_{CaS} after integration. Linear fitting revealed $R^2 = 0.991$, indicating g_A and g_{CaS} are highly correlated. Histograms in both pairwise correlation plots show the distribution of maximal conductances for both g_A and g_{CaS}. (E:) Variability in initial compartment mRNA level concentration of g_A vs. variability in g_A. Variability in g_A increases with variability in g_A channel mRNA concentration at a rate significantly lower than g_A channel mRNA concentration alone. (F:) Number of functional models vs. variability in g_A channel mRNA concentration.

It was then hypothesized that the scale of variability in initial maximal conductances and mRNA levels could contribute to patterns of ion channel correlations. We increased the variability in initial maximal conductances by a factor of 100, and in mRNA levels by a factor of 50. 1000 model neurons were initialized to quasi-random initial maximal conductances ranging between [0,500] and initial channel

mRNA concentrations ranging between [0,0.05]. Figure 3.4 shows the results of this experiment. It was found that a larger variation in initial conditions was not sufficient to reproduce the linear pairwise correlations between steady state channel maximal conductances, nor the variability in connection strengths observed experimentally. This indicated that initial conditions of the model neuron were not a significant influence on the emergence of ion channel correlations. Each model neuron underwent homeostatic regulation for $t = 200s$. As performed before, each model neuron was checked to ensure that the model converged to steady state maximal conductances, and had behavioral features which did not significantly differ from the reference bursting model neuron. The majority of model neurons produced target bursting behavior, showing that the integral control scheme is highly resistant to variation in these parameters. We can see that variability in maximal channel conductances increases with variability in channel mRNA concentration at a rate far lower than mRNA concentration alone. Most importantly, it was found that variability in these parameters resulted in compression of pairwise correlations between steady state maximal conductances from initial maximal conductances by a factor of 190, and that all versions of the model lie on a single point of the plane.

3.2 VARIABILITY IN PASSIVE ION LEAK CONDUCTANCE

We then moved on passive ion leak conductance (g_{leak}), which is unregulated in this model. It was hypothesized that though variability in regulated model parameters was insufficient to reproduce experimentally observed correlations, g_{leak} may have a significant influence because it is not regulated by the homeostatic rule.

Given that initial maximal conductances and channel mRNA concentrations were insufficient to reproduce experimentally observed variability in steady state channel maximal conductances, these parameters were allowed to vary between [0,5] and [0,0.001], respectively. g_{leak} was varied between [0,0.2] across all model neurons. g_{leak} was bound at 0.2 as the number of functional models after homeostatic regulation decreased significantly past this point.

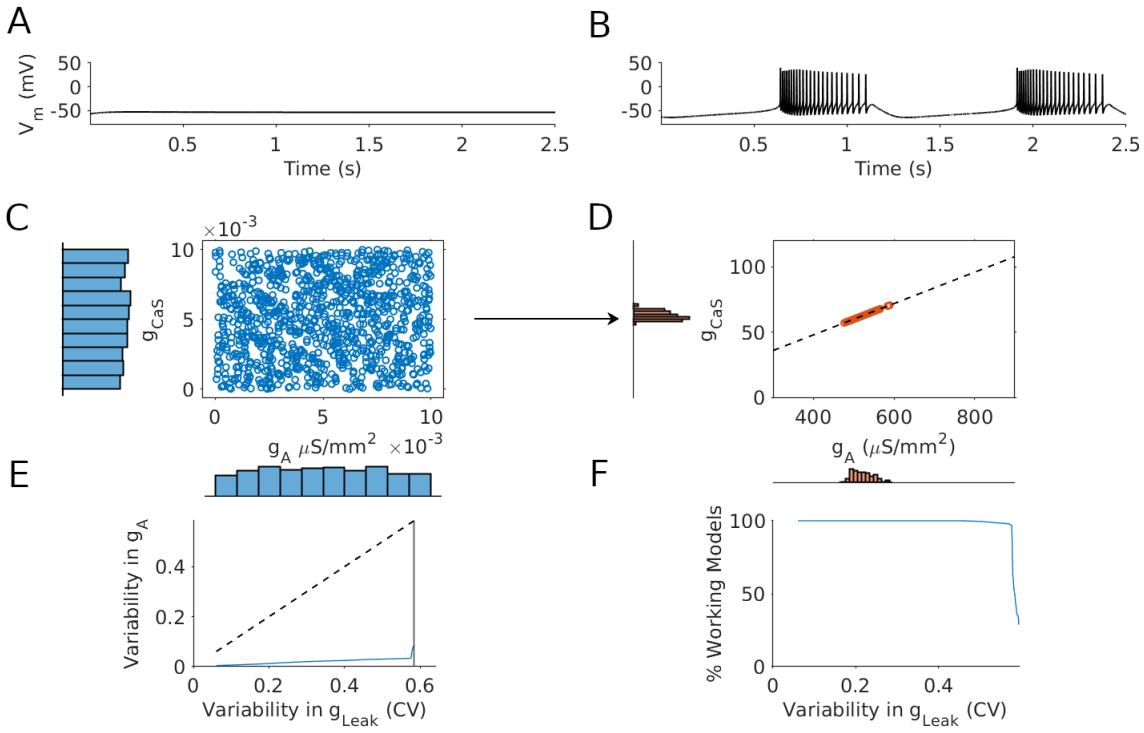

Figure 3.5: Variability in g_{leak} reproduces linear pairwise correlation between g_A and g_{CaS}. However, variation in maximal conductances is less than two-fold. CV for initial g_A is 0.583 and for steady state g_A is 0.00301, resulting in a compression factor of 120 when varying g_{leak} between [0,0.2]. (A-D:) Same as Figure 3.4. Linear fitting revealed $R^2 = 1$, indicating g_A and g_{CaS} are perfectly correlated. (E:) Variability in g_{leak} vs. variability in g_A. Variability in g_A increases with variability in g_{leak} at a rate significantly lower than g_{leak} alone. (F:) Number of functional models vs. variability in g_{leak}.

Figure 3.5 shows the results of the experiment. In stark contrast to a comparatively large variation in initial maximal conductances and channel mRNA levels, variation in g_{leak} was able to reproduce linear pairwise correlations between g_A and g_{CaS}. All solution sets of steady states maximal conductances in this experimental paradigm lie on a single plane taking the form of a line. However, despite greater than two-fold variability in g_{leak}, variation in steady state channel maximal conductances was less than two-fold, and was significantly compressed by the homeostatic rule with a compression factor of 120 between initial g_A and g_A after homeostatic regulation. Furthermore, variation in g_A increased at a rate significantly lower than g_{leak}, further cementing the compression in variability the homeostatic rule produced. It was determined that g_{leak} has a minor influence on the patterns of ion channel correlations that emerge from homeostatic regulation, but that variability in g_{leak} alone is not sufficient to reproduce the scale of

variability in experimentally observed correlations, nor the variability in connection strengths between maximal conductances.

3.3 VARIABILITY IN TARGET CA^{2+} CONCENTRATION

We then examined the features of the homeostatic tuning rule itself. We started off by varying Ca_{target}, positing that individual neurons may possess unique variability in target calcium concentration that can result in experimentally observed patterns of correlations while still producing target behavior. The experiment was set up in the same way as the previous experiment, with the same variation allowed in initial channel maximal conductances and mRNA concentrations. The distribution of Ca_{target} values was produced by scaling the reference value obtained from the Prinz *et al.* database described previously, and scaling it by a factor of 30. This scaling factor was produced by fine-tuning variation to ensure that a significant number of model neurons converged to bursting behavior after homeostatic regulation, but made sure that not all models converged so as to see the extreme ends of variation in this target.

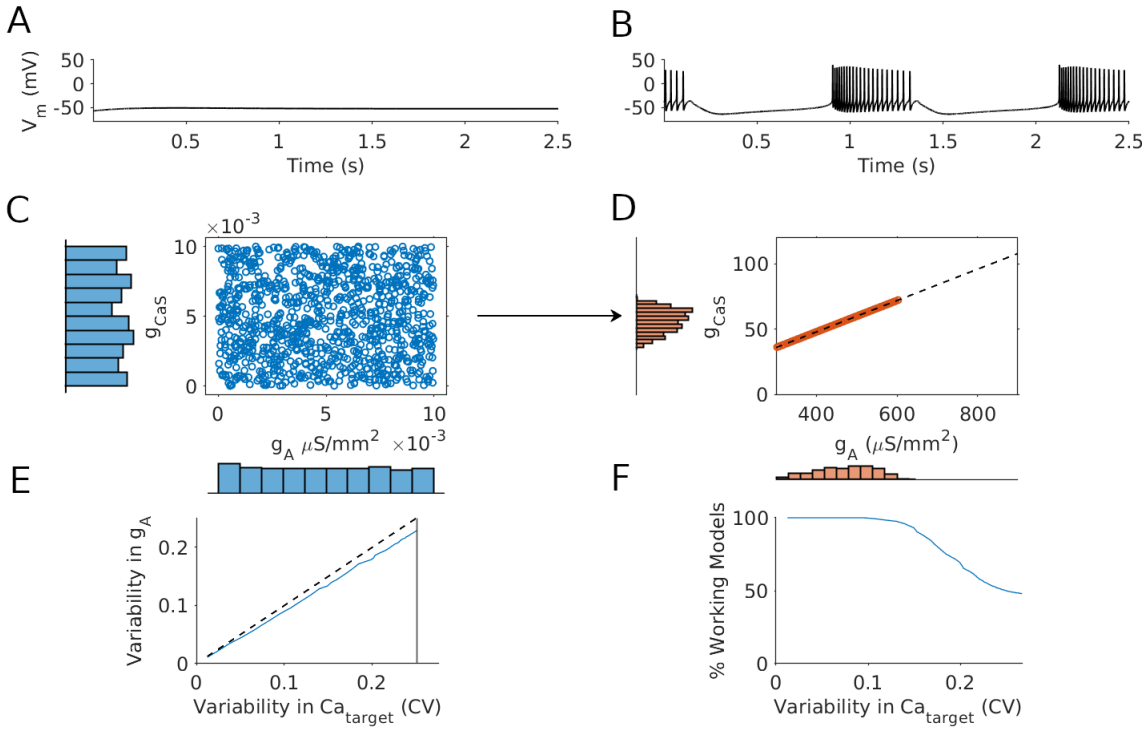

Figure 3.6: Variability in Ca_{target} reproduces linear pairwise correlation between g_A and g_{CaS}. Both g_A and g_{CaS} are shown to vary approximately two-fold, which is consistent with experimental evidence.[17] CV for initial g_A is 0.592 and for steady state g_A is 0.15, resulting in a compression factor of 4 when varying Ca_{target} between [24,198]. (A-D:) Same as Figure 3.4. Linear fitting revealed $R^2 = 1$, indicating g_A and g_{CaS} are perfectly correlated. (E:) Variability in Ca_{target} vs. variability in g_A. Variability in g_A increases with variability in Ca_{target} at a rate near equal to Ca_{target} alone. (F:) Number of functional models vs. variability in Ca_{target}.

After allowing model neurons to undergo homeostatic regulation, it was found that 30-fold variation in Ca_{target} reproduced linear pairwise correlations with approximately two-fold variation in steady state channel maximal conductances. It appears, then, that variability in Ca_{target} may play a significant role in reproducing experimentally observed correlations. However, variability in Ca_{target} alone was not sufficient to reproduce the variability in connection strengths observed experimentally[47]. Figure 3.6 shows the results of this experiment. It was found that increasing variability in Ca_{target} produced scaling of g_A that was nearly at the same rate as Ca_{target}. Along with that, variability in Ca_{target} resulted in significantly lower compression of steady state channel maximal conductances – a compression factor of only 4 was obtained by comparing the distribution of initial g_A to its steady state counterpart.

It thus became apparent that variability in homeostatic tuning rules, but not the components of the ion channels themselves, can result in

the emergence of experimentally observed variation in steady state channel maximal conductances.

3.4 VARIABILITY IN CONTROLLER TRANSLATION TIME CONSTANT

To fully explore this, we performed two more experiments, varying regulation time constants for transcription and translation independently. It was proposed that varying the transcription time constant, but not the translation time constant, would have a significant influence on observed patterns of correlation. This was assumed because the rate of translation is dependent on the rate of transcription – thus, the rate of transcription would determine the patterns of correlation. We began by initializing model neurons in the same manner as before, but varied τ_g between 4,000 and 6,000ms, independently for each ion channel, across 1000 model neurons.

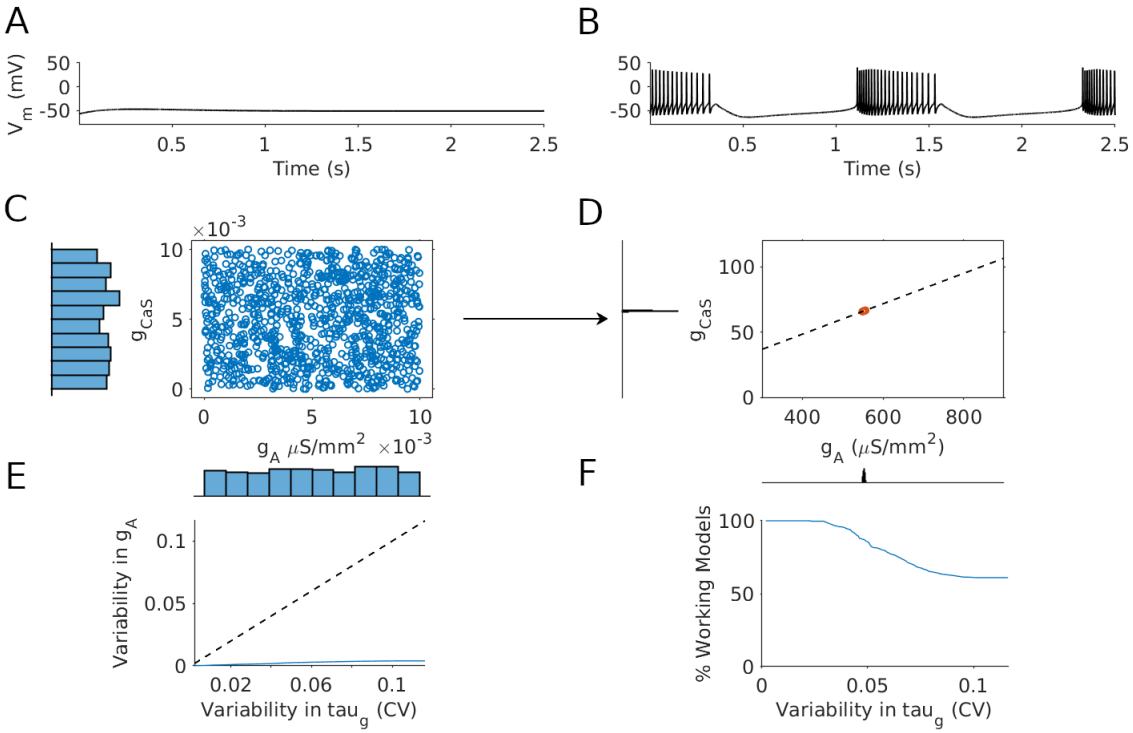

Figure 3.7: Variability in τ_g does not reproduce experimentally observed variation in maximal conductances. The pairwise correlation in steady state maximal conductances g_A and g_{CaS} exist as a single point on the plot. CV for initial g_A is 0.57 and for steady state g_A is 0.0029, resulting in a compression factor of 196 when varying τ_g for each channel between -1000 to 1000 milliseconds of its initial value described in Section 2.3. (A-D:) Same as Figure 3.4. Linear fitting revealed $R^2 = 0.978$, indicating g_A and g_{CaS} are highly correlated. (E:) Variability in τ_g vs. variability in g_A. Variability in g_A increases at a significantly lower rate than τ_g, which is consistent with the observed compression in variability of steady state maximal conductances. (F:) Number of functional models vs. variability in τ_g.

Figure 3.7 details the results of this experiment. Unsurprisingly, variation in τ_g was insufficient to reproduce the experimentally observed variation in steady state channel maximal conductances. It was found that the homeostatic tuning rule compressed variability in the steady state g_A distribution by a factor of 196 relative to the initial distribution. Variability in g_A increased at a rate far lower than τ_g, and all correlations between steady state channel maximal conductances were reduced to a single point on the plane.

This was an unsurprising result given that τ_g is not an independent parameter. Rather, it depends on the feedback from the transcription step in the homeostatic tuning rule – since the change in channel mRNA concentration determines the synthesis of ion channel pro-

teins, τ_g is thus determined to be dependent on the transcription rate constant, τ_m.

3.5 VARIABILITY IN CONTROLLER TRANSCRIPTION TIME CONSTANT

With this in mind, we decided to vary τ_m independently of other parameters, and independently for each ion channel. As was the case in all experiments, 1000 model neurons were initialized to aforementioned initial channel maximal conductances and channel mRNA concentrations. The transcription rate constant for each channel τ_m was allowed to vary between 1-1.5 times its initial value for each ion channel described in Section 2.3. An upper limit for the scaling of variation was determined by simulating variation in τ_m until a reasonable number of functional models was produced after homeostatic regulation.

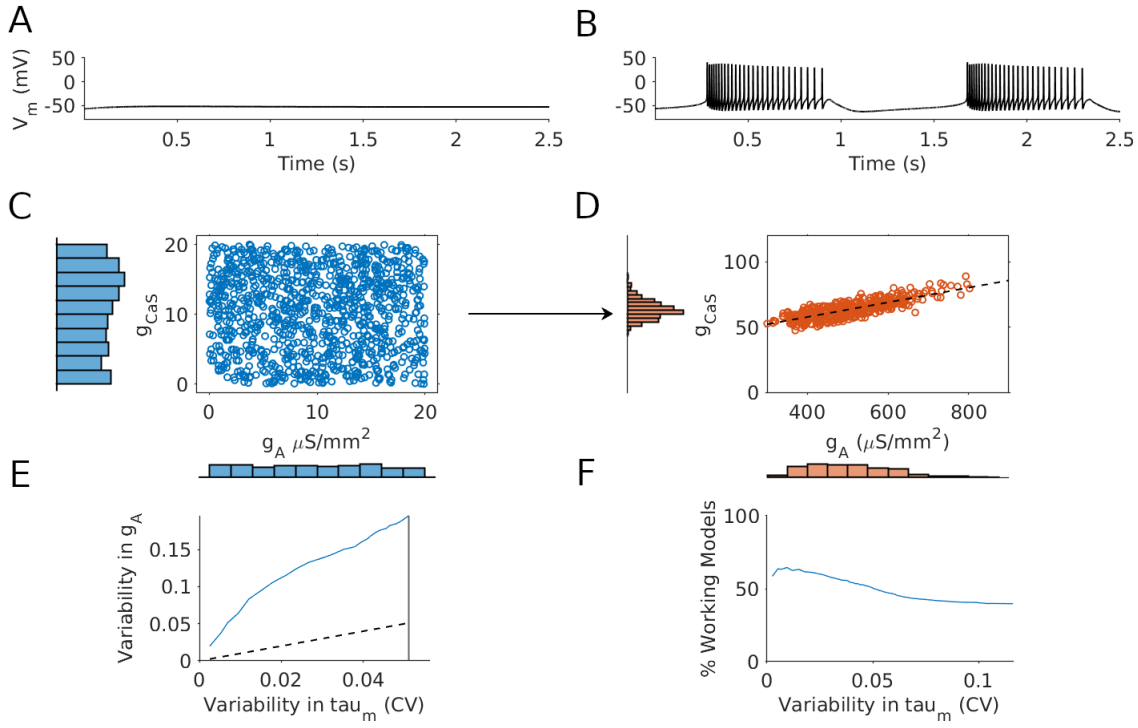

Figure 3.8: Variability in τ_m reproduces pairwise correlation between g_A and g_{CaS}. Both g_A and g_{CaS} are shown to vary greater than two-fold, which indicates that variability in τ_m can reproduce experimentally observed variation in maximal conductances.[17] CV for initial g_A is 0.585 and for steady state g_A is 0.198, resulting in a compression factor of 3 when varying τ_m for each channel between 1-1.5 times its initial value described in Section 2.3. (A-D:) Same as Figure 3.4. Linear fitting revealed $R^2 = 0.670$, indicating g_A and g_{CaS} are significantly correlated, but less so than in previous experiments. (E:) Variability in τ_m vs. variability in g_A. Variability in g_A increases with variability in τ_m at a rate far greater than τ_m alone. (F:) Number of functional models vs. variability in τ_m.

The results from this experiment were strikingly different from variations in all other parameters. Figure 3.8 shows that variation in τ_m for each ion channel resulted in pairwise correlations between steady state maximal conductances. More importantly, steady state maximal conductances were found to exist in an expanded solution space. Rather than all solutions existing on a single line, as in experiments varying Ca_{target} and g_{leak}, steady state maximal conductances were found to have a significantly larger spread. Variability in τ_m was interpreted to be capable of reproducing pairwise correlations between ion channels that varied in the range of experimentally observed correlations, and was able to reproduce correlations that were not perfect, as has been seen in experimental observations[47]. Linear fit of the pairwise correlation between the distribution of steady state g_A and g_{CaS} revealed $R^2 = 0.670$. In all other experiments, linear fit

revealed that 99%+ of the variation in one maximal conductance could be explained by another. Furthermore, the distribution of steady state maximal conductances was shown to be larger than two-fold for g_A and approximately two-fold for g_{CaS}, which is consistent with experimental observations where channel maximal conductances varied between two- to five-fold[17]. Variation in τ_m was also shown to result in increased variability in g_A relative to τ_m. In all other experiments, variation in steady state maximal conductances increased at a rate lower than the variability in the isolated parameter.

It has been made clear through systematic examination of parameters for both the components of the model neuron, as well as the homeostatic tuning rule, that variation in parameters of the homeostatic tuning rule itself can result in emergence of experimentally observed variation in steady state channel maximal conductances. Both variation in Ca_{target} and τ_m revealed significant pairwise correlations between steady state channel maximal conductances. Variation in τ_m revealed correlations between steady state channel maximal conductnaces that were not perfect, which is consistent with experimental observations[47].

4

CONCLUSION

Neurons are capable of processing and integrating an enormous variety of information, remaining sensitive to internal cues and modulatory biochemical and electrical inputs, while being robust to environmental perturbations and ion channel turnover. Neurons can maintain consistent patterns of activity despite variability within behaviorally equivalent types of neurons through activity-dependent feedback, a homeostatic regulatory mechanism which regulates channel mRNA levels and maximal conductances dependent on the firing rate activity of the neuron[24, 27, 55]. Activity-dependent feedback has been shown experimentally to produce compensatory changes in ion channel maximal conductance densities and mRNA concentrations after prolonged changes in firing rate activity. Furthermore, activity-dependent feedback has been shown to widen the range of characteristic sets of mRNA levels and conductance densities that can produce equivalent types of firing rate activity[16, 45].

Most important to this thesis, however, is how activity-dependent feedback as a process of homeostatic regulation can produce diverse, highly variable correlations between ion channels[17, 48, 49]. These correlations are ubiquitous across phyla, are genetically conserved, and are well documented across species and within cell types[30, 47, 48, 60, 61]. These correlations are important due to their ability to make neurons robust to environmental perturbations and ion channel turnover. Changes in maximal conductances of one ion channel can result in compensatory changes in others to preserve the activity of the neuron, indicating that these correlations allow for neurons to co-regulate ion channels – reducing the complexity of maintaining functional output within the cell. Co-regulation of ion channels makes neurons robust to perturbation by providing a mechanism by which neurons can up- or down-regulate ion channels dependent on the activity of its correlated channels.

Despite significant experimental observations across species and cell types, it is unknown how properties of ion channel correlations such as magnitude and connection strengths can emerge from homeostatic regulation. In this thesis, we explored how an activity-dependent feedback model based on the integral control scheme established by O'Leary *et al.* produces variability in magnitude and connection strengths of correlations between ion channels[36]. A systematic examination of the different intrinsic properties of neurons and the homeostatic regulatory mechanism was carried out. We first examined the magnitude of variability and strength of correlations between steady state maximal

conductances after variation in initial channel maximal conductance densities and mRNA levels. It was found that the model was highly insensitive to variability in initial conditions, compressed variability in steady state channel maximal conductances by a significant factor, and was unable to reproduce either the magnitude of variability between steady state channel maximal conductances or the strength of correlation between maximal conductances. We then examined the impact of variability in g_{leak} on these same properties of correlations between steady state channel maximal conductances. It was found that variability in the unregulated passive ion leak conductance was sufficient to reproduce a linear pairwise correlation between steady state maximal conductances, but the magnitude of variability was less than two-fold[17]. Along with that, all steady state maximal conductances were perfectly correlated.

It was thus determined that variability in magnitude and strength of correlations between ion channel maximal conductances was not significantly influenced by intrinsic properties of the neuron. Rather, variability in properties of the homeostatic regulatory mechanism significantly influences the magnitude of variability between maximal conductances and the strength of correlation. It was first shown that variability in Ca_{target} was sufficient to reproduce the magnitude of variability between steady state maximal conductances observed in experimental data. However, correlations between steady state maximal conductances were perfectly correlated, which is inconsistent with experimental observations which show varied connection strengths between ion channels[47]. Finally, the transcription and translation rate constants were varied to explore if these had any influence on the patterns of correlations between ion channels. It was unsurprising to find that variability in τ_g alone was insufficient to reproduce either the magnitude or connection strengths of correlations, given that the rate of translation into ion channel protein is dependent on the rate of mRNA transcription and concentration of channel mRNAs.

Variability in τ_m was sufficient to reproduce the experimentally observed magnitude in variation within ion channel maximal conductance distributions and strengths of correlation between ion channel maximal conductances. While in all other simulations, if linear pairwise correlations were produced at all, channel maximal conductances were perfectly correlated. In contrast, varying τ_m produced correlations where changes in one channel could not be fully explained by changes in another. Variability in rates of transcription, but not any other parameters, reproduced the full range of properties of correlations found in experimental observations[47–49]. Thus, it has been shown that robust and diverse correlations can emerge from homeostatic tuning rules and variability in the rates of transcription of ion channel mRNAs.

BIBLIOGRAPHY

[1] Annarosa Arcangeli. "Ion channels and transporters in cancer. 3. Ion channels in the tumor cell-microenvironment cross talk." In: *American Journal of Physiology. Cell Physiology* 301.4 (Oct. 2011), pp. C762–771. ISSN: 1522-1563. DOI: 10.1152/ajpcell.00113.2011.

[2] John M. Ball, Clarence C. Franklin, Anne-Elise Tobin, David J. Schulz, and Satish S. Nair. "Coregulation of Ion Channel Conductances Preserves Output in a Computational Model of a Crustacean Cardiac Motor Neuron." In: *The Journal of Neuroscience* 30.25 (June 23, 2010), pp. 8637–8649. ISSN: 0270-6474. DOI: 10.1523/JNEUROSCI.6435-09.2010. URL: https://www.ncbi.nlm.nih.gov/pmc/articles/PMC4473856/ (visited on 12/08/2019).

[3] Deborah J. Baro, Robert M. Levini, Marshall T. Kim, Allan R. Willms, Cathy Cole Lanning, Hilda E. Rodriguez, and Ronald M. Harris-Warrick. "Quantitative Single-Cell-Reverse Transcription-PCR Demonstrates That A-Current Magnitude Varies as a Linear Function ofshal Gene Expression in Identified Stomatogastric Neurons." In: *Journal of Neuroscience* 17.17 (Sept. 1, 1997), pp. 6597–6610. ISSN: 0270-6474, 1529-2401. DOI: 10.1523/JNEUROSCI.17-17-06597.1997. URL: https://www.jneurosci.org/content/17/17/6597 (visited on 12/17/2019).

[4] Magnus Baumgardt, Irene Miguel-Aliaga, Daniel Karlsson, Helen Ekman, and Stefan Thor. "Specification of Neuronal Identities by Feedforward Combinatorial Coding." In: *PLOS Biology* 5.2 (Feb. 6, 2007), e37. ISSN: 1545-7885. DOI: 10.1371/journal.pbio.0050037. URL: https://journals.plos.org/plosbiology/article?id=10.1371/journal.pbio.0050037 (visited on 12/17/2019).

[5] Sharon Bergquist, Dion K. Dickman, and Graeme W. Davis. "A Hierarchy of Cell Intrinsic and Target-Derived Homeostatic Signaling." In: *Neuron* 66.2 (Apr. 29, 2010), pp. 220–234. ISSN: 0896-6273. DOI: 10.1016/j.neuron.2010.03.023. URL: https://www.ncbi.nlm.nih.gov/pmc/articles/PMC2864777/ (visited on 12/17/2019).

[6] William J. Blake, Mads KAErn, Charles R. Cantor, and J. J. Collins. "Noise in eukaryotic gene expression." In: *Nature* 422.6932 (Apr. 10, 2003), pp. 633–637. ISSN: 0028-0836. DOI: 10.1038/nature01546.

[7] Denis Burdakov, Oleg Gerasimenko, and Alexei Verkhratsky. "Physiological Changes in Glucose Differentially Modulate the Excitability of Hypothalamic Melanin-Concentrating Hormone and Orexin Neurons In Situ." In: *Journal of Neuroscience* 25.9 (Mar. 2, 2005), pp. 2429–2433. ISSN: 0270-6474, 1529-2401. DOI: 10.1523/JNEUROSCI.4925-04.2005. URL: https://www.jneurosci.org/content/25/9/2429 (visited on 12/17/2019).

[8] Robert H. Cudmore and Gina G. Turrigiano. "Long-term potentiation of intrinsic excitability in LV visual cortical neurons." In: *Journal of Neurophysiology* 92.1 (July 2004), pp. 341–348. ISSN: 0022-3077. DOI: 10.1152/jn.01059.2003.

[9] Gaël Daoudal and Dominique Debanne. "Long-term plasticity of intrinsic excitability: learning rules and mechanisms." In: *Learning & Memory (Cold Spring Harbor, N.Y.)* 10.6 (Dec. 2003), pp. 456–465. ISSN: 1072-0502. DOI: 10.1101/lm.64103.

[10] Graeme W. Davis. "Homeostatic control of neural activity: from phenomenology to molecular design." In: *Annual Review of Neuroscience* 29 (2006), pp. 307–323. ISSN: 0147-006X. DOI: 10.1146/annurev.neuro.28.061604.135751.

[11] Peter Dayan. *Theoretical neuroscience : computational and mathematical modeling of neural systems*. Cambridge, Mass: Massachusetts Institute of Technology Press, 2001. ISBN: 9780262041997.

[12] N. S. Desai, L. C. Rutherford, and G. G. Turrigiano. "Plasticity in the intrinsic excitability of cortical pyramidal neurons." In: *Nature Neuroscience* 2.6 (June 1999), pp. 515–520. ISSN: 1097-6256. DOI: 10.1038/9165.

[13] Niraj S. Desai. "Homeostatic plasticity in the CNS: synaptic and intrinsic forms." In: *Journal of Physiology, Paris* 97.4 (Nov. 2003), pp. 391–402. ISSN: 0928-4257. DOI: 10.1016/j.jphysparis.2004.01.005.

[14] René A. W. Frank. "Endogenous ion channel complexes: the NMDA receptor." In: *Biochemical Society Transactions* 39.3 (June 2011), pp. 707–718. ISSN: 1470-8752. DOI: 10.1042/BST0390707.

[15] JL Franklin, DJ Fickbohm, and AL Willard. "Long-term regulation of neuronal calcium currents by prolonged changes of membrane potential." In: *The Journal of Neuroscience* 12.5 (May 1, 1992), pp. 1726–1735. ISSN: 0270-6474. DOI: 10.1523/JNEUROSCI.12-05-01726.1992. URL: https://www.ncbi.nlm.nih.gov/pmc/articles/PMC6575878/ (visited on 05/06/2020).

[16] Mark S. Goldman, Jorge Golowasch, Eve Marder, and L. F. Abbott. "Global Structure, Robustness, and Modulation of Neuronal Models." In: *Journal of Neuroscience* 21.14 (July 15, 2001), pp. 5229–5238. ISSN: 0270-6474, 1529-2401. DOI: 10.1523/JNEUROSCI.

21-14-05229.2001. URL: https://www.jneurosci.org/content/21/14/5229 (visited on 12/17/2019).

[17] J. Golowasch, L. F. Abbott, and E. Marder. "Activity-dependent regulation of potassium currents in an identified neuron of the stomatogastric ganglion of the crab Cancer borealis." In: *The Journal of Neuroscience: The Official Journal of the Society for Neuroscience* 19.20 (Oct. 15, 1999), RC33. ISSN: 1529-2401.

[18] Srinivas Gorur-Shandilya, Alec Hoyland, and Eve Marder. "Xolotl: An Intuitive and Approachable Neuron and Network Simulator for Research and Teaching." In: *Frontiers in Neuroinformatics* 12 (2018). Publisher: Frontiers. ISSN: 1662-5196. DOI: 10.3389/fninf.2018.00087. URL: https://www.frontiersin.org/articles/10.3389/fninf.2018.00087/full (visited on 05/09/2020).

[19] Rodolfo J. Haedo and Jorge Golowasch. "Ionic Mechanism Underlying Recovery of Rhythmic Activity in Adult Isolated Neurons." In: *Journal of Neurophysiology* 96.4 (Oct. 1, 2006), pp. 1860–1876. ISSN: 0022-3077. DOI: 10.1152/jn.00385.2006. URL: https://www.physiology.org/doi/full/10.1152/jn.00385.2006 (visited on 12/17/2019).

[20] A. L. Hodgkin and A. F. Huxley. "A quantitative description of membrane current and its application to conduction and excitation in nerve." In: *The Journal of Physiology* 117.4 (Aug. 28, 1952), pp. 500–544. ISSN: 0022-3751. URL: https://www.ncbi.nlm.nih.gov/pmc/articles/PMC1392413/ (visited on 05/09/2020).

[21] A. L. Hodgkin and A. F. Huxley. "The components of membrane conductance in the giant axon of Loligo." In: *The Journal of Physiology* 116.4 (Apr. 28, 1952), pp. 473–496. ISSN: 0022-3751. URL: https://www.ncbi.nlm.nih.gov/pmc/articles/PMC1392209/ (visited on 05/06/2020).

[22] A. L. Hodgkin, A. F. Huxley, and B. Katz. "Measurement of current-voltage relations in the membrane of the giant axon of Loligo." In: *The Journal of Physiology* 116.4 (Apr. 28, 1952), pp. 424–448. ISSN: 0022-3751. URL: https://www.ncbi.nlm.nih.gov/pmc/articles/PMC1392219/ (visited on 05/06/2020).

[23] Jonghwan Kim, Jianlin Chu, Xiaohua Shen, Jianlong Wang, and Stuart H. Orkin. "An extended transcriptional network for pluripotency of embryonic stem cells." In: *Cell* 132.6 (Mar. 21, 2008), pp. 1049–1061. ISSN: 1097-4172. DOI: 10.1016/j.cell.2008.02.039.

[24] G. LeMasson, E. Marder, and L. F. Abbott. "Activity-dependent regulation of conductances in model neurons." In: *Science (New York, N.Y.)* 259.5103 (Mar. 26, 1993), pp. 1915–1917. ISSN: 0036-8075. DOI: 10.1126/science.8456317.

[25] Zheng Li, Ken-Ichi Okamoto, Yasunori Hayashi, and Morgan Sheng. "The importance of dendritic mitochondria in the morphogenesis and plasticity of spines and synapses." In: *Cell* 119.6 (Dec. 17, 2004), pp. 873–887. ISSN: 0092-8674. DOI: 10.1016/j.cell.2004.11.003.

[26] B. Liss, O. Franz, S. Sewing, R. Bruns, H. Neuhoff, and J. Roeper. "Tuning pacemaker frequency of individual dopaminergic neurons by Kv4.3L and KChip3.1 transcription." In: *The EMBO journal* 20.20 (Oct. 15, 2001), pp. 5715–5724. ISSN: 0261-4189. DOI: 10.1093/emboj/20.20.5715.

[27] Zheng Liu, Jorge Golowasch, Eve Marder, and L. F. Abbott. "A Model Neuron with Activity-Dependent Conductances Regulated by Multiple Calcium Sensors." In: *Journal of Neuroscience* 18.7 (Apr. 1, 1998), pp. 2309–2320. ISSN: 0270-6474, 1529-2401. DOI: 10.1523/JNEUROSCI.18-07-02309.1998. URL: https://www.jneurosci.org/content/18/7/2309 (visited on 12/17/2019).

[28] Sven Loebrich and Elly Nedivi. "The function of activity-regulated genes in the nervous system." In: *Physiological Reviews* 89.4 (Oct. 2009), pp. 1079–1103. ISSN: 0031-9333. DOI: 10.1152/physrev.00013.2009.

[29] Jason N. MacLean, Ying Zhang, Marie L. Goeritz, Richard Casey, Ricardo Oliva, John Guckenheimer, and Ronald M. Harris-Warrick. "Activity-independent coregulation of IA and Ih in rhythmically active neurons." In: *Journal of Neurophysiology* 94.5 (Nov. 2005), pp. 3601–3617. ISSN: 0022-3077. DOI: 10.1152/jn.00281.2005.

[30] Jason N. MacLean, Ying Zhang, Bruce R. Johnson, and Ronald M. Harris-Warrick. "Activity-independent homeostasis in rhythmically active neurons." In: *Neuron* 37.1 (Jan. 9, 2003), pp. 109–120. ISSN: 0896-6273. DOI: 10.1016/s0896-6273(02)01104-2.

[31] Eve Marder and Jean-Marc Goaillard. "Variability, compensation and homeostasis in neuron and network function." In: *Nature Reviews. Neuroscience* 7.7 (July 2006), pp. 563–574. ISSN: 1471-003X. DOI: 10.1038/nrn1949.

[32] Eve Marder and Kristina J. Rehm. "Development of central pattern generating circuits." In: *Current Opinion in Neurobiology* 15.1 (Feb. 2005), pp. 86–93. ISSN: 0959-4388. DOI: 10.1016/j.conb.2005.01.011.

[33] Céline Marionneau, Yarimar Carrasquillo, Aaron J. Norris, R. Reid Townsend, Lori L. Isom, Andrew J. Link, and Jeanne M. Nerbonne. "The Sodium Channel Accessory Subunit Nav1 Regulates Neuronal Excitability through Modulation of Repolarizing Voltage-Gated K+ Channels." In: *The Journal of Neuroscience* 32.17 (Apr. 25, 2012), pp. 5716–5727. ISSN: 0270-6474. DOI: 10.1523/

JNEUROSCI.6450-11.2012. URL: https://www.ncbi.nlm.nih.gov/pmc/articles/PMC3347704/ (visited on 12/17/2019).

[34] Hiroaki Misonou, Milena Menegola, Durga P. Mohapatra, Lauren K. Guy, Kang-Sik Park, and James S. Trimmer. "Bidirectional Activity-Dependent Regulation of Neuronal Ion Channel Phosphorylation." In: *Journal of Neuroscience* 26.52 (Dec. 27, 2006), pp. 13505–13514. ISSN: 0270-6474, 1529-2401. DOI: 10.1523/JNEUROSCI.3970-06.2006. URL: https://www.jneurosci.org/content/26/52/13505 (visited on 12/17/2019).

[35] Hiroaki Misonou, Durga P. Mohapatra, Eunice W. Park, Victor Leung, Dongkai Zhen, Kaori Misonou, Anne E. Anderson, and James S. Trimmer. "Regulation of ion channel localization and phosphorylation by neuronal activity." In: *Nature Neuroscience* 7.7 (July 2004), pp. 711–718. ISSN: 1097-6256. DOI: 10.1038/nn1260.

[36] Timothy O'Leary, Alex H. Williams, Jonathan S. Caplan, and Eve Marder. "Correlations in ion channel expression emerge from homeostatic tuning rules." In: *Proceedings of the National Academy of Sciences* 110.28 (July 9, 2013), E2645–E2654. ISSN: 0027-8424, 1091-6490. DOI: 10.1073/pnas.1309966110. URL: https://www.pnas.org/content/110/28/E2645 (visited on 12/08/2019).

[37] Timothy O'Leary, Alex H. Williams, Alessio Franci, and Eve Marder. "Cell types, network homeostasis, and pathological compensation from a biologically plausible ion channel expression model." In: *Neuron* 82.4 (May 21, 2014), pp. 809–821. ISSN: 1097-4199. DOI: 10.1016/j.neuron.2014.04.002.

[38] Timothy O'Leary, Mark C W van Rossum, and David J A Wyllie. "Homeostasis of intrinsic excitability in hippocampal neurones: dynamics and mechanism of the response to chronic depolarization." In: *The Journal of Physiology* 588 (Pt 1 Jan. 1, 2010), pp. 157–170. ISSN: 0022-3751. DOI: 10.1113/jphysiol.2009.181024. URL: https://www.ncbi.nlm.nih.gov/pmc/articles/PMC2821556/ (visited on 05/06/2020).

[39] I.-Feng Peng and Chun-Fang Wu. "Drosophila cacophony channels: a major mediator of neuronal Ca2+ currents and a trigger for K+ channel homeostatic regulation." In: *The Journal of Neuroscience: The Official Journal of the Society for Neuroscience* 27.5 (Jan. 31, 2007), pp. 1072–1081. ISSN: 1529-2401. DOI: 10.1523/JNEUROSCI.4746-06.2007.

[40] Astrid A. Prinz, Cyrus P. Billimoria, and Eve Marder. "Alternative to hand-tuning conductance-based models: construction and analysis of databases of model neurons." In: *Journal of Neurophysiology* 90.6 (Dec. 2003), pp. 3998–4015. ISSN: 0022-3077. DOI: 10.1152/jn.00641.2003.

[41] Astrid A. Prinz, Dirk Bucher, and Eve Marder. "Similar network activity from disparate circuit parameters." In: *Nature Neuroscience* 7.12 (Dec. 2004), pp. 1345–1352. ISSN: 1097-6256. DOI: 10.1038/nn1352.

[42] Joseph L. Ransdell, Satish S. Nair, and David J. Schulz. "Rapid Homeostatic Plasticity of Intrinsic Excitability in a Central Pattern Generator Network Stabilizes Functional Neural Network Output." In: *Journal of Neuroscience* 32.28 (July 11, 2012), pp. 9649–9658. ISSN: 0270-6474, 1529-2401. DOI: 10.1523/JNEUROSCI.1945-12.2012. URL: https://www.jneurosci.org/content/32/28/9649 (visited on 12/17/2019).

[43] Kristina J. Rehm, Katherine E. Deeg, and Eve Marder. "Developmental Regulation of Neuromodulator Function in the Stomatogastric Ganglion of the Lobster, Homarus americanus." In: *The Journal of Neuroscience* 28.39 (Sept. 24, 2008), pp. 9828–9839. ISSN: 0270-6474. DOI: 10.1523/JNEUROSCI.2328-08.2008. URL: https://www.ncbi.nlm.nih.gov/pmc/articles/PMC2614700/ (visited on 12/17/2019).

[44] Kristina J. Rehm, Adam L. Taylor, Stefan R. Pulver, and Eve Marder. "Spectral analyses reveal the presence of adult-like activity in the embryonic stomatogastric motor patterns of the lobster, Homarus americanus." In: *Journal of Neurophysiology* 99.6 (June 2008), pp. 3104–3122. ISSN: 0022-3077. DOI: 10.1152/jn.00042.2008.

[45] Edmund W. Rodgers, Wulf-Dieter Krenz, Xiaoyue Jiang, Lingjun Li, and Deborah J. Baro. "Dopaminergic tone regulates transient potassium current maximal conductance through a translational mechanism requiring D1Rs, cAMP/PKA, Erk and mTOR." In: *BMC Neuroscience* 14.1 (Nov. 13, 2013), p. 143. ISSN: 1471-2202. DOI: 10.1186/1471-2202-14-143. URL: https://doi.org/10.1186/1471-2202-14-143 (visited on 12/17/2019).

[46] L. K. Samuels. *In Defense of Chaos: the Chaology of Politics, Economics and Human Action*. Cobden Press, 2013.

[47] Joseph M. Santin and David J. Schulz. "Membrane Voltage Is a Direct Feedback Signal That Influences Correlated Ion Channel Expression in Neurons." In: *Current Biology* 29 (2019), 1683–1688.e2. DOI: 10.1016/j.cub.2019.04.008.

[48] David J. Schulz, Jean-Marc Goaillard, and Eve E. Marder. "Quantitative expression profiling of identified neurons reveals cell-specific constraints on highly variable levels of gene expression." In: *Proceedings of the National Academy of Sciences of the United States of America* 104.32 (Aug. 7, 2007), pp. 13187–13191. ISSN: 0027-8424. DOI: 10.1073/pnas.0705827104.

[49] David J. Schulz, Jean-Marc Goaillard, and Eve Marder. "Variable channel expression in identified single and electrically coupled neurons in different animals." In: *Nature Neuroscience* 9.3 (Mar. 2006), pp. 356–362. ISSN: 1097-6256. DOI: 10.1038/nn1639.

[50] David J. Schulz and Brian J. Lane. "Homeostatic Plasticity of Excitability in Crustacean Central Pattern Generator Networks." In: *Current opinion in neurobiology* 43 (Apr. 2017), pp. 7–14. ISSN: 0959-4388. DOI: 10.1016/j.conb.2016.09.015. URL: https://www.ncbi.nlm.nih.gov/pmc/articles/PMC5382137/ (visited on 05/07/2020).

[51] Mala M. Shah, Rebecca S. Hammond, and Dax A. Hoffman. "Dendritic ion channel trafficking and plasticity." In: *Trends in Neurosciences* 33.7 (July 2010), pp. 307–316. ISSN: 1878-108X. DOI: 10.1016/j.tins.2010.03.002.

[52] Gongyi Shi, Kensuke Nakahira, Scott Hammond, Kenneth J Rhodes, Lee E Schechter, and James S Trimmer. "Subunits Promote K+ Channel Surface Expression through Effects Early in Biosynthesis." In: *Neuron* 16.4 (Apr. 1, 1996), pp. 843–852. ISSN: 0896-6273. DOI: 10.1016/S0896-6273(00)80104-X. URL: http://www.sciencedirect.com/science/article/pii/S089662730080104X (visited on 12/17/2019).

[53] Wafa Soofi, Santiago Archila, and Astrid A. Prinz. "Co-variation of ionic conductances supports phase maintenance in stomatogastric neurons." In: *Journal of Computational Neuroscience* 33.1 (Aug. 2012), pp. 77–95. ISSN: 1573-6873. DOI: 10.1007/s10827-011-0375-3.

[54] Wolfgang Stein. "Modulation of stomatogastric rhythms." In: *Journal of Comparative Physiology. A, Neuroethology, Sensory, Neural, and Behavioral Physiology* 195.11 (Nov. 2009), pp. 989–1009. ISSN: 1432-1351. DOI: 10.1007/s00359-009-0483-y.

[55] M. Stemmler and C. Koch. "How voltage-dependent conductances can adapt to maximize the information encoded by neuronal firing rate." In: *Nature Neuroscience* 2.6 (June 1999), pp. 521–527. ISSN: 1097-6256. DOI: 10.1038/9173.

[56] Andrew M. Swensen and Bruce P. Bean. "Robustness of Burst Firing in Dissociated Purkinje Neurons with Acute or Long-Term Reductions in Sodium Conductance." In: *Journal of Neuroscience* 25.14 (Apr. 6, 2005), pp. 3509–3520. ISSN: 0270-6474, 1529-2401. DOI: 10.1523/JNEUROSCI.3929-04.2005. URL: https://www.jneurosci.org/content/25/14/3509 (visited on 12/17/2019).

[57] Anne M. Taylor, Nicole C. Berchtold, Victoria M. Perreau, Christina H. Tu, Noo Li Jeon, and Carl W. Cotman. "Axonal mRNA in uninjured and regenerating cortical mammalian axons." In: *The Journal of Neuroscience: The Official Journal of the Society for Neuro-*

science 29.15 (Apr. 15, 2009), pp. 4697–4707. ISSN: 1529-2401. DOI: 10.1523/JNEUROSCI.6130-08.2009.

[58] Simone Temporal, Mohati Desai, Olga Khorkova, Gladis Varghese, Aihua Dai, David J. Schulz, and Jorge Golowasch. "Neuromodulation independently determines correlated channel expression and conductance levels in motor neurons of the stomatogastric ganglion." In: *Journal of Neurophysiology* 107.2 (Oct. 12, 2011), pp. 718–727. ISSN: 0022-3077. DOI: 10.1152/jn.00622.2011. URL: https://www.physiology.org/doi/full/10.1152/jn.00622.2011 (visited on 12/08/2019).

[59] Simone Temporal, Kawasi M. Lett, and David J. Schulz. "Activity-dependent feedback regulates correlated ion channel mRNA levels in single identified motor neurons." In: *Current biology: CB* 24.16 (Aug. 18, 2014), pp. 1899–1904. ISSN: 1879-0445. DOI: 10.1016/j.cub.2014.06.067.

[60] Anne-Elise Tobin, Nelson D. Cruz-Bermúdez, Eve Marder, and David J. Schulz. "Correlations in Ion Channel mRNA in Rhythmically Active Neurons." In: *PLOS ONE* 4.8 (Aug. 25, 2009), e6742. ISSN: 1932-6203. DOI: 10.1371/journal.pone.0006742. URL: https://journals.plos.org/plosone/article?id=10.1371/journal.pone.0006742 (visited on 12/08/2019).

[61] Trinh Tran, Cagri T. Unal, Daniel Severin, Laszlo Zaborszky, Horacio G. Rotstein, Alfredo Kirkwood, and Jorge Golowasch. "Ionic current correlations are ubiquitous across phyla." In: *Scientific Reports* 9.1 (Feb. 8, 2019), pp. 1–9. ISSN: 2045-2322. DOI: 10.1038/s41598-018-38405-6. URL: https://www.nature.com/articles/s41598-018-38405-6 (visited on 12/08/2019).

[62] G. G. Turrigiano. "Homeostatic plasticity in neuronal networks: the more things change, the more they stay the same." In: *Trends in Neurosciences* 22.5 (May 1999), pp. 221–227. ISSN: 0166-2236. DOI: 10.1016/s0166-2236(98)01341-1.

[63] G. G. Turrigiano, K. R. Leslie, N. S. Desai, L. C. Rutherford, and S. B. Nelson. "Activity-dependent scaling of quantal amplitude in neocortical neurons." In: *Nature* 391.6670 (Feb. 26, 1998), pp. 892–896. ISSN: 0028-0836. DOI: 10.1038/36103.

[64] G. Turrigiano, L. F. Abbott, and E. Marder. "Activity-dependent changes in the intrinsic properties of cultured neurons." In: *Science (New York, N.Y.)* 264.5161 (May 13, 1994), pp. 974–977. ISSN: 0036-8075. DOI: 10.1126/science.8178157.

[65] G. Turrigiano, G. LeMasson, and E. Marder. "Selective regulation of current densities underlies spontaneous changes in the activity of cultured neurons." In: *The Journal of Neuroscience: The Official Journal of the Society for Neuroscience* 15.5 (May 1995), pp. 3640–3652. ISSN: 0270-6474.

[66] Gina G. Turrigiano and Sacha B. Nelson. "Homeostatic plasticity in the developing nervous system." In: *Nature Reviews. Neuroscience* 5.2 (Feb. 2004), pp. 97–107. ISSN: 1471-003X. DOI: 10.1038/nrn1327.

[67] Carlos G. Vanoye, Richard C. Welch, Changlin Tian, Charles R. Sanders, and Alfred L. George. "KCNQ1/KCNE1 assembly, co-translation not required." In: *Channels (Austin, Tex.)* 4.2 (Apr. 2010), pp. 108–114. ISSN: 1933-6969. DOI: 10.4161/chan.4.2.11141.

[68] Dmitri Volfson, Jennifer Marciniak, William J. Blake, Natalie Ostroff, Lev S. Tsimring, and Jeff Hasty. "Origins of extrinsic variability in eukaryotic gene expression." In: *Nature* 439.7078 (Feb. 16, 2006), pp. 861–864. ISSN: 1476-4687. DOI: 10.1038/nature04281.

[69] Wei Zhang and David J. Linden. "The other side of the engram: experience-driven changes in neuronal intrinsic excitability." In: *Nature Reviews Neuroscience* 4.11 (Nov. 2003), pp. 885–900. ISSN: 1471-0048. DOI: 10.1038/nrn1248. URL: https://www.nature.com/articles/nrn1248 (visited on 12/17/2019).

[70] Yili Zhang and Jorge Golowasch. "Recovery of rhythmic activity in a central pattern generator: analysis of the role of neuromodulator and activity-dependent mechanisms." In: *Journal of computational neuroscience* 31.3 (Nov. 2011), pp. 685–699. ISSN: 0929-5313. DOI: 10.1007/s10827-011-0338-8. URL: https://www.ncbi.nlm.nih.gov/pmc/articles/PMC4459654/ (visited on 12/17/2019).

DECLARATION

I declare that all work in this thesis is my own. Code for this project is available at https://github.com/btromm/neuralcorr-thesis

Waltham, Massachusetts, May 2020

Robert Tromm

COLOPHON

This document was typeset using the typographical look-and-feel `classicthesis` developed by André Miede and Ivo Pletikosić. The style was inspired by Robert Bringhurst's seminal book on typography "*The Elements of Typographic Style*".